The epileptogenic trinity

Oxidative stress, brain inflammation and iron in epilepsy

Zimmer, T.S.

Publication date
2021

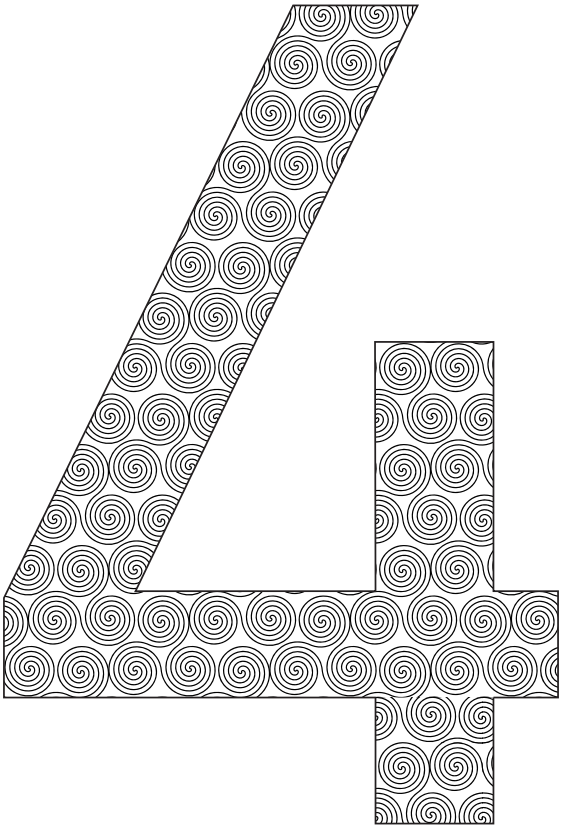

UPREGULATION OF THE PATHOGENIC TRANSCRIPTION FACTOR SPI1/PU.1 IN TUBEROUS SCLEROSIS COMPLEX AND FOCAL CORTICAL DYSPLASIA BY OXIDATIVE STRESS

Till S. Zimmer[1], Anatoly Korotkov[1], Susan Zwakenberg[2], Floor E. Jansen[3], Fried J. T. Zwartkruis[2], Nicholas R. Rensing[5], Michael Wong[5], Angelika Mühlebner[1,4], Erwin A. van Vliet[1,6], Eleonora Aronica[1,7,*], James D. Mills[1,8,9,*]

[1]Amsterdam UMC, University of Amsterdam, Department of (Neuro)Pathology, Amsterdam Neuroscience, Amsterdam, the Netherlands
[2]University Medical Center Utrecht, Center for Molecular Medicine, Molecular Cancer Research, Utrecht, the Netherlands
[3]University Medical Center Utrecht, Department of Pediatric Neurology, Brain Center, Utrecht, the Netherlands
[4]Department of Pathology, University Medical Center Utrecht, Utrecht, the Netherlands
[5]Washington University, Department of Neurology, Saint Louis, MO, United States of America
[6]University of Amsterdam, Swammerdam Institute for Life Sciences, Center for Neuroscience, Amsterdam, the Netherlands
[7]Stichting Epilepsie Instellingen Nederland (SEIN), Heemstede, the Netherlands
[8]Department of Clinical and Experimental Epilepsy, UCL, London, United Kingdom
[9]Chalfont Centre for Epilepsy, Chalfont St Peter, United Kingdom

*shared last authorship

Brain Pathol.* (2021), *accepted for publication

Abstract

Tuberous sclerosis complex (TSC) is a congenital disorder characterized by cortical malformations and concomitant epilepsy due to loss-of-function mutations in the mTOR suppressors TSC1 or TSC2. While the underlying molecular changes due to mTOR activation in TSC have previously been investigated, the drivers of these transcriptional change have not been fully elucidated. A better understanding of the perturbed transcriptional regulation could lead to the identification of novel pathways for therapeutic intervention not only in TSC, but other genetic epilepsies in which mTOR activation plays a key role, such as focal cortical dysplasia II (FCD).

Here, we analysed RNA-sequencing data from cortical tubers and from a *tsc2*$^{-/-}$ zebrafish. Using these datasets, we identified conserved differential expression of several transcription factors (TFs), including SPI1/PU.1, along with conserved enrichment of differentially expressed gene targets. Next, we confirmed overexpression of SPI1/PU.1 on the RNA and protein level in a separate cohort of surgically resected TSC tubers and FCD tissue, in fetal TSC tissue and a *Tsc1*$^{GFAP-/-}$ mouse model of TSC. Subsequently, we validated the expression of SPI1/PU.1 in dysmorphic cells with mTOR activation in TSC tubers. In fetal TSC, we detected SPI1/PU.1 expression prenatally and elevated RNA Spi1 expression in *Tsc1*$^{GFAP-/-}$ mice before the development of seizures. Finally, *in vitro*, we identified that in astrocytes and neurons SPI1 transcription was driven by H_2O_2-induced oxidative stress, independent of mTOR.

We identified SPI1/PU.1 as a novel TF involved in the pro-inflammatory gene expression of malformed cells in TSC and FCD IIb. This transcriptional program is activated in response to oxidative stress and already present prenatally. Importantly, SPI1/PU.1 protein appears to be strictly limited to malformed cells, as we did not find SPI1/PU.1 protein in mice nor in our *in vitro* models.

Abbreviations

FCD = focal cortical dysplasia, TSC = tuberous sclerosis complex, TF = transcription factor, GO = gene ontology, RNA-Seq = RNA-sequencing, OS = oxidative stress, SPI1/PU.1 = SPI1 proto-oncogene/Purine rich box 1, mTOR = mammalian target of rapamycin, mTORC1 = mTOR complex 1, NF-κB = nuclear factor kappa-light-chain-enhancer of activated B cells, tp53 = tumor protein 53, SPI1/PU.1 = SPI1 Proto-Oncogene/purine-rich box 1, IRF8 = Interferon Regulatory Factor 8, GBX2 = Gastrulation Brain Homeobox 2, IKZF1 = IKAROS Family Zinc Finger 1, RELB = RELB proto-oncogene, RELA = RELA proto-oncogene, REL = REL proto-oncogene, GO = gene ontology, ISH = *in situ* hybridization, DAB = 3,3'-diaminobenzidine, AEC = 3'-amino 9'-ethylcarbazole

Keywords: tuberous sclerosis complex, focal cortical dysplasia, epilepsy, mTOR, brain inflammation, oxidative stress

Introduction

Tuberous sclerosis complex (TSC) is a genetic disorder that is caused in part by loss-of-function mutations in one of two genes, TSC1 or TSC2. The proteins encoded from these genes, tuberin and hamartin, are important regulators of the mammalian target of rapamycin complex 1 (mTORC1) (10). As such, loss of function mutations in these genes can lead to the hyperactivation of the mTOR pathway resulting in unregulated cell growth and proliferation across numerous organs (3, 10). This multisystem disorder presents with a wide range of clinical manifestations of which the most debilitating affect the central nervous system and include neurodevelopmental delay, autism, and severe seizures (13, 14). Focal cortical malformations, known as cortical tubers, are present in the brains of approximately 90 % of patients with TSC and are thought to represent the epileptogenic foci and thus drivers of seizure activity (13, 32). Histological examination of resected cortical tubers reveals a severely distorted cortex, with the apparent loss of cortical layers and heterogeneous entities consisting of a variety of abnormal cell-types, including dysmorphic neurons, giant cells and reactive astrocytes (11). For approximately a third of patients it is possible to manage the seizure activity successfully with anti-epileptic drugs. The remaining group of patients frequently undergo surgical resection of the cortical tubers. After surgery, 57 % of TSC patients achieve seizure freedom and another 18 % show a significant reduction in seizure frequency within the first-year post-surgery (29, 34). However, for approximately 25 % of patients there is no reduction in seizure frequency, and for 3 % of these cases there are significant associated surgical morbidities (62). With the current treatments targeted at suppressing seizure activity being of mixed effectiveness, there is an urgent need to better understand the cellular and molecular signatures of the epileptogenic brain lesions in TSC so that appropriate treatments can be applied.

At the molecular level, TSC cortical tubers are characterised by an inflammatory response, and activation of the immune system, along with disruption of the extracellular matrix and the blood-brain barrier (42, 71). Further, emerging evidence suggests that oxidative stress (OS) may also play a major role in TSC pathology and the subsequent epileptogenesis (2, 15, 46, 60, 64, 80). The exact role of these processes in the pathological manifestations of TSC has not been fully elucidated, nor have the important regulatory drivers. However, current studies point to complex and intricate regulatory networks involving interactions and interplay between microRNAs, loss of heterozygosity, DNA-methylation changes and transcriptional regulation (9, 12, 23, 24, 42, 58). Besides the transcription factors (TFs) tumor protein p53 (tp53) and nuclear factor kappa-light-chain-enhancer of activated B cells (NF-κB), little attention has been given to potential transcriptional control of the TSC-associated genes (2, 16, 37).

A closely related pathology, which presents as one of the leading causes of refractory childhood epilepsies, is focal cortical dysplasia (FCD) (28). Of all the FCD subtypes, FCD type IIb presents striking histopathological similarities with TSC, such as dysmorphic neurons, dysplastic glia and balloon cells, which closely resemble giant cells in TSC upon microscopic examination (44). Importantly, FCDs are caused by germline or somatic mutations in regulators of mTOR itself, ultimately resulting in mTOR hyperactivity similar to TSC (4). Therefore, FCD and TSC are classified as mTORopathies, characterized by malformed cortical development and frequent epilepsy, likely representing a spectrum of diseases along the mTOR pathway (43). Consequently, TSC could serve as model disease to better understand the pathogenesis of mTORopathies and these insights could also be extrapolated to novel treatments for FCDs.

In this study, by leveraging previously published RNA-sequencing (RNA-Seq) data, we aim to identify TFs that are important regulators of the perturbed gene expression patterns seen in TSC cortical tubers and to investigate if these changes can be extrapolated to FCD IIb. Subsequently, using *in vitro* and *in vivo* models along with resected human brain tissue we delineate the relationship between mTOR activation, the cortical tuber micro-environment, and the activation of the TFs of interest.

Materials & Methods

Subjects

Surgical and post-mortem brain tissue was selected from the archives of the Neuropathology of the Amsterdam University Medical Centres (Amsterdam UMC, location Academic Medical Center (AMC), Amsterdam, the Netherlands), and the University Medical Center Utrecht (UMCU, Utrecht, the Netherlands). Cortical brain samples from patients diagnosed with FCD IIb or TSC were obtained from brain surgery for intractable epilepsy. Informed consent was acquired for the use of brain tissue for research purposes. Diagnostic workup of the obtained brain specimens was performed by two neuropathologists independently. The diagnosis of FCD was confirmed according to the international consensus classification system proposed for grading FCD (5). All patients with cortical tubers fulfilled the diagnostic criteria for TSC (53), while none of the FCD patients fulfilled the diagnostic criteria for TSC. Control material was obtained at autopsy from age-matched controls, without a history of seizures or other neurological diseases. All autopsies were performed within 24 h after death. Tissue was obtained and used in accordance with the Declaration of Helsinki and the Amsterdam UMC Research Code provided by the Medical Ethics Committee and approved by the science committee of the UMC Utrecht Biobank. Clinical information about the brain samples used in this study are summarized in Suppl. Table 1 and 2.

RNA-sequencing data

The final differential expression outputs from two different RNA-sequencing (RNA-Seq) experiments were provided by the data generators on request (42, 57). Dataset 1 was a comparison between TSC cortical tuber (n=12) and matched controls (n=10), dataset 2 was comparison between *tsc2*$^{-/-}$ zebrafish (n=4) and wildtype (n=4). For full details on RNA-sequencing protocols used and differential expression analysis we refer to the relevant papers.

Transcription factor enrichment analysis

The transcription factors (TFs) that were amongst the genes up-regulated in TSC cortical tubers from the aforementioned RNA-Seq analysis were taken for further analysis. The TFs tp53 and NF-κB, although not up-regulated at the gene level, were also included as they have previously been associated with TSC. First, all target genes for each TF were extracted from the ChIP-X database (36). The ChiP-X database consists of gene-TF relationships inferred from ChIP-chip, ChIP-Seq, ChIP-PET and DamID experiments. Of the NF-κB family members, RELB proto-oncogene (RELB), RELA proto-oncogene (RELA), nuclear factor kappa B subunit 1 (NFKB1), nuclear factor kappa B subunit 2 (NFKB2), and REL proto-oncogene (REL), only RELA appeared in the ChiP-X database so it was used to assess NF-κB binding potential. Next, the up-regulated genes were assessed for over-representation of target genes for each TF using hypergeometric testing. The gene list was considered enriched for TF targets when the p-value was < 0.05.

To assess the up-regulated genes in the *tsc2*$^{-/-}$ zebrafish for enrichment of gene targets for the same set of TFs, a similar approach was employed. First, the target genes listed for each TF was converted to zebrafish homologs using BioMart (17, 18). Using the converted gene targets the up-regulated genes were assessed for over-representation of target genes for each TF using hypergeometric testing. The gene list was considered enriched for TF targets when the p-value was < 0.05.

Pathway and gene ontology enrichment analysis

The genes that were up-regulated when TSC cortical tubers were compared to control tissue, were passed to the R package ReactomePA for pathway enrichment analysis (76). The ReactomePA package allows for enrichment analysis using the reactome pathway database (31). Those pathways with a Benjamini-Hochberg adjusted p-value < 0.05 were considered significant.

The up-regulated genes that were targets of each TF of interest were passed to the R package clusterProfiler for a gene ontology (GO) overrepresentation enrichment analysis (77). The genes were assessed for enrichment at the GO levels of “cellular compartment”, “biological process”, and “molecular function”. Those GO with a Benjamini-Hochberg adjusted p-value < 0.05 were considered significant.

Tsc1$^{GFAP-/-}$ mice

All animal experiments in this study were approved by the Washington University Animal Welfare committee. *Tsc1*$^{flox/flox-GFAP}$-Cre knockout (*Tsc1*$^{GFAP-/-}$) mice with conditional inactivation of the Tsc1 gene in astrocytes and neurons were generated as described previously (68). *Tsc1*$^{flox/+-GFAP}$-Cre and Tsc1flox/flox littermates have previously been found to have no abnormal phenotype and were used as controls in these experiments. Whole cortex and hippocampus were collected from 2-week-old and 2-month-old animals (n=5 animals per group). While 2-week-old *Tsc1*$^{GFAP-/-}$ mice do not have any neurological abnormalities and seizures yet, 2-month-old animals typically present with chronic recurrent seizures (19). For quantitative real-time PCR, tissues were mechanically minced and homogenized in Qiazol Lysis Reagent (Qiagen Benelux, Venlo, the Netherlands). Subsequent RNA isolation was done using the miRNeasy Mini kit (Qiagen Benelux, Venlo, the Netherlands) according to the manufacturer's instructions.

Immunohistochemistry on human and mouse brain tissue

Human brain tissue was either snap frozen in liquid nitrogen and stored at -80 °C for RNA analysis or fixed in 10 % neutral buffered formalin and embedded in paraffin for immunohistochemistry. Paraffin embedded tissue was sectioned at 5 µm, mounted on pre-coated glass slides (Star Frost, Waldemar Knittel Glasbearbeitungs, Braunschweig, Germany) and used for immunohistochemical stainings. Sections were deparaffinated in xylene, and ethanol (100 %, 96 %) and incubated for 20 min in 0.3 % H_2O_2 diluted in methanol, to block any residual endogenous peroxidase activity. Antigen retrieval was performed using a pressure cooker in 0.01 M sodium citrate buffer (pH 6.0) at 121 °C for 10 min. This was followed by washes in phosphate buffered saline (PBS; 0.1 M, pH 7.4) and incubation with primary antibody against SPI1 (SPI1/PU.1; rabbit monoclonal, clone EP18, Bio SB, Santa Barbara, CA, USA; 1:100) or immune regulatory factor 8 (IRF8; mouse monoclonal, clone E9, Santa Cruz, Dallas, TX, USA; 1:50) in antibody diluent (VWR International, Radnor, PA, USA) at 4°C overnight. The next day, sections were washed in PBS and then stained with a polymer-based peroxidase immunohistochemistry detection kit (Brightvision plus kit, ImmunoLogic, Duiven, the Netherlands) according to the manufacturer's instructions. Staining was performed using Bright 3,3'-diaminobenzidine (DAB) substrate solution (ImmunoLogic, Duiven, the Netherlands). The reaction was stopped by washing twice in distilled water. Finally, sections were counterstained with Haematoxylin-Mayer solution (Klinipath, Breda, the Netherlands), dehydrated in alcohol and xylene, and coverslipped using Pertex (VWR International, Radnor, PA, USA).

Double-labelling of SPI/PU.1 was performed with neuronal nuclear protein (NeuN; mouse monoclonal, clone MAB377; Merck-Millipore, Temecula, CA, USA; 1:2000), histocompatibility complex II (HLA-DR; mouse monoclonal, Agilent, Santa Clara, CA, USA; 1:100), ionized calcium-binding adapter molecule 1 (Iba-1; rabbit polyclonal,

WAKO, Osaka, Japan, 1:2000), glial fibrillary acidic protein (GFAP; mouse monoclonal, clone GA5, Sigma-Aldrich, St. Louis, MO, USA; 1:4000), phosphorylated S6 ribosomal protein (pS6; rabbit monoclonal, clone 91B2, Cell Signaling Technologies, Danvers, MA, USA; 1:100) or nitric oxide synthase 2 (iNOS; rabbit polyclonal, Abcam, Cambridge, UK; 1:250). For red and blue IHC, sections were incubated at 4°C overnight with SPI1 primary antibody. The next day, sections were washed with PBS and incubated with BrightVision poly-alkaline phosphatase (AP) anti-rabbit (Immunologic, Duiven, the Netherlands) for 30 min at room temperature and again washed with PBS. AP activity was visualized with the AP substrate kit III Vector Blue (SK-5300, Vector Laboratories Inc., Burlingame, CA, USA). Subsequently, sections were cooked in citrate buffer and then washed with PBS. Incubation with anti-pS6 antibody was performed at 4 °C overnight in antibody diluent (VWR International, Radnor, PA, USA). Sections were processed with a Brightvision kit as described in the preceding text for 30 min at room temperature. Staining was developed using 3'-amino 9'-ethylcarbazole substrate solution (AEC, Sigma-Aldrich, St. Louis, MO, USA). Sections incubated without the primary antibody were essentially blank.

For immunofluorescent labelling, sections were incubated with the respective primary antibodies overnight in antibody diluent (VWR International, Radnor, PA, USA) at 4 °C. The next day, sections were washed with PBS and incubated with Alexa Fluor 568 goat anti-rabbit and Alexa Fluor 488 donkey anti-mouse antibody (Invitrogen, Eugene, OR, USA, 1:200) in antibody diluent (VWR International, Radnor, PA, USA) for 2 hours at room temperature, mounted with Vectashield (Vector Laboratories Inc., Burlingame, CA, USA) and visualized using Leica Confocal Microscope TCS SP8 X DLS (Leica, Son, the Netherlands) at 200x magnification (bidirectional X, speed 600 Hz, pinhole 1.00 AU).

For Spi1/Pu.1 cell count in *Tsc1*$^{GFAP-/-}$ mice, 2 pictures from each hemisphere per animal in the posterior parietal association area were taken. Cells were manually counted and are plotted as total cell count per animal from both hemispheres.

In situ hybridization

Paraffin-embedded brain tissue was deparaffinised and underwent antigen retrieval as described in the previous paragraph. The oligonucleotide probe for Spi1 (Suppl. Table 3) contained LNA modification, 2-o-methyl modification and a digoxygenin (DIG) label (Qiagen Benelux, Venlo, the Netherlands). Sections were incubated with 100 nM of the probe in hybridization mix (600 mM NaCl, 10 mM HEPES, 1 mM EDTA, 5x Denhardts, 50 % Formamide) for 90 min at 56 °C. Sections were washed with 2x saline-sodium citrate (SSC) for 2 min, 0.5x SSC for 2 min and 0.2x SSC for 1 min. After washing with sterile PBS, sections were blocked for 15 min with 1 % bovine serum albumin, 0.02 % Tween 20 and 1 % normal goat serum (NGS). Hybridization was detected with AP labelled anti-DIG (Roche Applied Science, Basel, Switzerland).

Nitro-blue tetrazolium chloride (NBT)/5-bromo-4-chloro-3-indolyl phosphate p-toluidine salt (BCIP) was used as chromogenic substrate for AP (1:50 diluted in NTM-T buffer (100 mM Tris, pH 9.5; 100 mM NaCl; 50 mM $MgCl_2$; 0.05 % Tween 20). For double labelling, slides were developed with Vector blue substrate instead. Thereafter, slides were blocked with 10 % NGS in PBS for 30 min at room temperature followed by antibody and AEC development as described. Negative control assays were performed without probes (sections were blank).

RNA isolation & quantitative real-time PCR

For RNA isolation, human tissues as well as cell culture material were homogenized in 700 µL Qiazol Lysis Reagent (Qiagen Benelux, Venlo, the Netherlands). Total RNA was isolated using the miRNeasy Mini kit (Qiagen Benelux, Venlo, the Netherlands) according to the manufacturer's instructions. The concentration and purity of RNA was determined at 260/280 nm using a Nanodrop spectrophotometer (Thermo Fisher Scientific, Wilmington, DE, USA). For quantitative real-time PCR, 250 ng of cell culture derived total RNA or 500 ng tissue-derived total RNA were reverse-transcribed into cDNA using oligo-dT primers. Quantitative PCRs were run on a Roche Lightcycler 480 thermocycler (Roche Applied Science, Basel, Switzerland) using the reference genes chromosome 1 open reading frame 43 (C1ORF43) and elongation factor 1-α (EF1α) for human mRNA and hypoxanthine phosphoribosyltransferase 1 (Hprt) and TATA-Box binding protein (Tbp) for mouse mRNA (Suppl Table 4 for primer sequences). Quantification of data was performed using LinRegPCR as described elsewhere (69).

Cell cultures

Primary fetal astrocyte-enriched cell cultures were obtained from human fetal brain tissue (cortex, 14–19 gestational weeks) from medically induced abortions. All material was collected from donors from whom written informed consent for the use of the material for research purposes was obtained by the Bloemenhove kliniek (Heemstede, the Netherlands). Tissue was obtained in accordance with the Declaration of Helsinki and the Amsterdam UMC Research Code provided by the Medical Ethics Committee. Cell isolation was performed as described previously (69). Briefly, large blood vessels were removed, after which the tissue was mechanically minced into smaller fragments. Tissue was enzymatically digested by incubating at 37 °C for 30 min with 2.5 % trypsin (Sigma-Aldrich, St. Louis, MO, USA). Tissue was washed with incubation medium containing Dulbecco's modified Eagle's medium (DMEM)/HAM F10 (1:1) medium (Thermo Fisher Scientific, Waltham, MA, USA), supplemented with 100 units/mL penicillin, 100 µg/mL streptomycin, 1 % glutamine (Thermo Fisher Scientific, Waltham, MA, USA) and 10 % fetal calf serum (FCS; Thermo Fisher Scientific, Waltham, MA, USA) and triturated by passing through a 70 µm mesh filter. The cell suspension was incubated at 37 °C, 5 % CO_2 for 48 h to let glial cells adhere to the culture flask before it was washed with PBS to remove excess of myelin and cell debris.

SH-SY5Y cells were cultured in DMEM/HAM F-12 supplemented with 100 units/mL penicillin, 100 µg/mL streptomycin and 10 % FCS. Cultures were subsequently refreshed twice a week. Primary cultures reached confluence after 2–3 weeks.
TSC cultures were derived from surgical brain tissue (cortex) obtained from patients undergoing epilepsy surgery at the Wilhelmina Children's Hospital of the University Medical Center Utrecht (UMCU, Utrecht, the Netherlands). All cases were reviewed and diagnosed as described in the preceding text. Cultures were established and cultured in the same manner as fetal astrocyte-enriched cultures.

Cell cultures for experiments were obtained by trypsinizing confluent cultures and sub-plating onto poly-L-lysine (PLL, 15 µg/mL, Sigma-Aldrich, St. Louis, MO, USA)-precoated 12-well plates (Greiner Bio-One, Kremsmünster, Austria); $5x10^4$ cells/well for RNA isolation and PCR. TSC-derived astrocyte cultures were used at passage 2-5 for all experiments. Human fetal astrocytes were treated with 500 µM of H_2O_2 for varying periods (Sigma-Aldrich, St Louis, MO, USA), 100nM Rapamycin (VWR International, Radnor, PA, USA) or 10 ng/mL recombinant IL-1β for 24h (PeproTech, Rocky Hill, NJ, USA) in complete culture medium at 37 °C and 5 % CO_2. SH-SY5Y cells were treated with indicated concentrations H_2O_2 for 3h in culture medium containing 1 % FCS. For rapamycin treatment, rapamycin was applied 1 hour in advance of the 6 hour H_2O_2 stimulation.

Statistical analysis

Statistical analysis was performed with GraphPad Prism software version 5.01 (Graphpad software Inc., La Jolla, CA, USA) using the non-parametric Mann-Whitney U test or Kruskal-Walli test followed by Dunn *post hoc* analysis for multiple groups. $P<0.05$ was assumed to indicate a significant difference. Correlation analysis was performed using Spearman's rank correlation. Data is displayed as bar graphs with standard deviation (SD) or Tukey style box plot with interquartile range from 25th to 75th percentile plus outliers.

Results

Identification of SPI1/PU.1 as a pathogenic regulator of the TSC cortical tuber transcriptional network

To identify transcriptional activators that are putative regulators of the TSC cortical tuber transcriptional network, we reanalysed the RNA-sequencing (RNA-Seq) data outputs produced by Mills et al. 2017 (42). In this study, 269 genes were identified as up-regulated (adjusted p-value < 0.05) and 169 genes were identified as down-regulated (adjusted p-value < 0.05) in the TSC cortical tubers when compared to controls (Figure 1A). The 269 up-regulated genes were assessed for the presence

of genes associated with the GO term: DNA-binding transcription factor activity (GO:0003700). Amongst the twenty-four up-regulated genes that appeared in this GO term five encode for transcription factors (TFs), of which four also appear in the ChIP-X database (36). Based on this, the TFs SPI1 Proto-Oncogene (SPI1/PU.1), Interferon Regulatory Factor 8 (Irf8), Gastrulation Brain Homeobox 2 (Gbx2), and IKAROS Family Zinc Finger 1 (Ikzf1) were selected for further analysis (Figure 1A). Of these TFs, at the gene level, SPI1 had the highest expression in TSC cortical tubers (17.91 fragments per kilobase million (fpkm)), followed by IRF8 (10.78 fpkm), while GBX2 (1.18 fpkm) and IKZF1 (1.89 fpkm) were both expressed at low levels (Figure 1B).

Next, the genes up-regulated in the TSC cortical tubers were assessed for enrichment of target genes for each of the four selected TFs. Based on the ChIP-X database, of the 269 up-regulated genes SPI1/PU.1 was a putative transcriptional activator of 136, Irf8 targeted 24, and Ikzf1 and Gbx2 were predicted to be involved in the transcriptional regulation of 4 and 2 genes, respectively (Table 1). Interestingly, 18 of the 24 gene targets of Irf8 were also predicted targets of SPI1/PU.1. Subsequently, hypergeometric testing was performed to assess if there was a significant enrichment of gene targets for each TF; the up-regulated genes were significantly enriched for SPI1/PU.1 (p-value = $2.10x10^{-7}$) and Irf8 (p-value = 0.0009) gene targets, but not for Gbx2 (p-value = 0.56) or Ikzf1 (p-value = 0.08) targets. By comparison the genes that form the NF-κB protein complex, RELB proto-oncogene (RELB), RELA proto-oncogene (RELA), nuclear factor kappa B subunit 1 (NFKB1), nuclear factor kappa B subunit 2 (NFKB2), and REL proto-oncogene (REL) along with TP53 were not differentially expressed, and the TFs themselves were predicted to target 73 (p-value = $1.23 x10^{-7}$) and 36 genes of the differentially expressed gene set (p-value = 0.06), respectively (Supplementary Figure 1A, Table 1).

Subsequently, the expression of SPI1 was correlated with the expression of its putative target genes. Of the 136 target genes, SPI1/PU.1 was highly correlated ($\rho > 0.70$, p-value < 0.05) with 99 including complement C1q B chain (C1QB) ($\rho = 0.948$), complement C3 (C3) ($\rho = 0.908$), triggering receptor expressed on myeloid cells 2 (TREM2) ($\rho = 0.879$), interleukin 1 beta (IL1B) ($\rho = 0.817$), and IRF8 ($\rho = 0.87$). To assess the function of the 136 putative target genes, a gene ontology (GO) enrichment analysis was performed at the level of cellular compartment, biological process, and molecular function. The top enriched GO terms for each level included terms related to the extracellular matrix, immune processes, inflammatory terms, alterations to receptor activity and binding (Figure 1C).

Next, a reactome pathway enrichment analysis of the up-regulated genes was performed. In total 39 pathways were identified as enriched (adjusted p-value < 0.05) the majority of which were related to inflammation and immune responses. To

Table 1: Summary of differentially expressed transcription factors from human TSC tubers and *tsc2*$^{-/-}$ brain tissue

Human (Control Tissue v TSC cortical Tubers)							Zebrafish (WT v tsc2$^{-/-}$)					
Transcription Factor	Description	log_2(FC)	adjusted p-value	Target Genes (Expressed)	Target Genes (Up-regulated)	Enrichment p-value	Ortholog	log_2(FC)	adjusted p-value	Target Genes (Expressed)	Target Genes (Up-regulated)	Enrichment p-value
Spi1/PU.1	SPI1 proto-oncogene	1.607	0.016	6020	136	2.10E-07	spi1b	1.431	0.041	6170	737	4.31E-23
Irf8	Interferon regulatory factor 8	2.184	0.004	754	24	0.0009	irf8	0.572	0.224	720	78	0.039
Gbx2	Gastrulation brain homeobox 2	3.360	0.039	185	2	0.56	gbx2	0.017	0.986	197	6	0.999
Ikzf1	Ikaros family zinc finger	1.230	0.004	101	4	0.08	ikzf1	0.962	0.039	143	16	0.202
Tp53	Tumor protein p53	0.268	0.967	3930	73	0.068	tp53	0.572	0.010	4362	353	0.999
Rel	REL Proto-Oncogene, NF-KB Subunit	-0.296	0.925	NA	NA	NA	rel	-0.682	0.020	NA	NA	NA
Rela	RELA Proto-Oncogene, NF-KB Subunit	0.074	0.998	870	36	1.24E-07	rela	-0.694	0.431	967	117	0.014
Relb	RELB Proto-Oncogene, NF-KB Subunit	0.720	0.511	NA	NA	NA	relb	0.663	0.049	NA	NA	NA
Nfkb1	Nuclear Factor Kappa B Subunit 1	0.340	0.860	NA	NA	NA	nfkb1	0.032	0.983	NA	NA	NA
Nfkb2	Nuclear Factor Kappa B Subunit 2	0.508	0.752	NA	NA	NA	nfkb2	0.288	0.332	NA	NA	NA

evaluate which of the enriched reactome pathways may be under the transcriptional control of one of the TFs of interest, the number of gene targets of each TF in each pathway were assessed. All top 20 enriched pathways had multiple (number of genes > 1) SPI1/PU.1 gene targets, while Irf8, Ikzf1 and Gbx2 targeted 2, 1 and 0 pathways, respectively (Figure 1D). In comparison, tp53 had multiple gene targets in 19 pathways and NF-κB had multiple gene targets in 14 pathways.

Finally, by leveraging a RNA-Seq analysis of a TSC zebrafish model by Scheldeman et al. 2017, we assessed the conservation of the TFs of interest across an *in vivo* model of TSC (57). Of the zebrafish homologs of the four TFs of interest, the SPI1 homolog spi1b (adjusted p-value = 0.041) (Supplementary Figure 1B) along with the IKZF1 homolog ikzf1 (adjusted p-value = 0.039) were up-regulated in the TSC zebrafish model. The expression of the zebrafish homologs of GBX2 and IRF8 did not differ (Supplementary Figure 1B). After converting the target genes extracted from the ChIP-X database to their zebrafish homologs, the up-regulated genes in the TSC zebrafish model were assessed for enrichment of TF targets. Of the 1820 genes up-regulated in the TSC zebrafish model, spi1b targeted 737, irf8 targeted 78 genes, while ikzf1 and gbx2 16 and 6 genes, respectively (Table 1). Hypergeometric testing revealed an enrichment for spi1b (p-value = $4.3x10^{-23}$) and irf8 gene targets (p-value = 0.0388), while there was no enrichment for target genes of gbx2 and ikzf1. Again, the TFs tp53 and NF-κB were assessed at the gene expression level in the TSC zebrafish model, tp53 was up-regulated (adjusted p-value = 0.01) along with the NF-κB family member rel (adjusted p-value = 0.0486). However, the expression of the members rela (adjusted p-value = 0.43), nfkb1 (adjusted p-value = 0.98), and nfkb2 (adjusted p-value = 0.33) did not differ, while the expression of family member relb was lower (adjusted p-value = 0.02) (Supplementary Figure 1C). In terms of transcriptional control, tp53 was predicted to target 353 (p-value = 0.999) of the up-regulated genes and NF-κB was predicted to target 117 (p-value= 0.014) of the up-regulated genes (Table 1).
Based on the up-regulation of SPI1 in the RNA-Seq data, enrichment of correlated gene targets amongst the up-regulated genes, the predicted involvement in pathways relevant to TSC molecular pathogenesis, along with the conservation of expression patterns and enrichment of target genes in the TSC zebrafish model, we decided to focus predominately on the TF SPI1/PU.1.

SPI1/PU.1 is localized in malformed cells in TSC cortical tubers and FCD IIb foci

After identifying SPI1/PU.1 as a key transcriptional regulator in TSC tubers, we validated its expression in TSC tuber tissue and the closely related mTORopathy FCD IIb. In autoptic control tissue, SPI1/PU.1 expression was restricted exclusively to microglial nuclei (Figure 2A, A_1 arrowheads). In contrast, dysmorphic neurons and balloon/giant cells (referred to as malformed cells) in FCD and TSC displayed

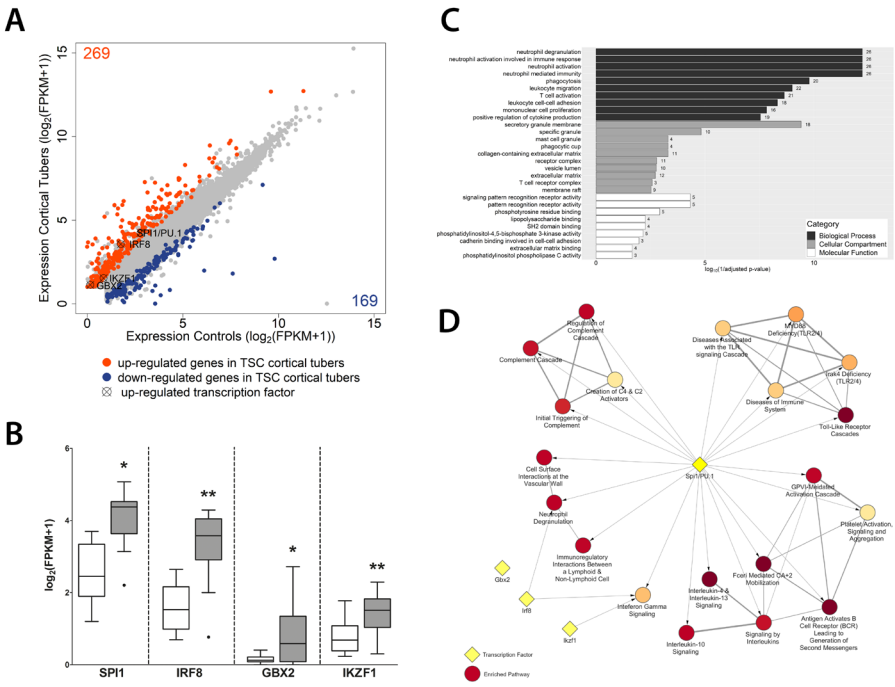

Figure 1: Identification of SPI1, IRF8, GBX2 and IKZF1 as novel transcription factors in TSC cortical tuber. Differential expression analysis of cortical tuber tissue vs. age-matched cortical control samples derived from autopsy revealed 269 upregulated (orange) and 169 downregulated (blue) genes. Four potentially important transcriptional regulators were identified from the upregulated genes (cross circle) (A). Comparison of log_2FPKM values from cortical tuber tissue versus age matched cortical control tissue from autopsy (B). GO enrichment analysis of the top 10 enriched pathways of 139 genes predicted to be targeted by SPI1/PU.1 identified predominantly immune system associated GO terms (C). Reactome pathway enrichment analysis of the up-regulated genes from RNA-Seq revealed SPI1/PU.1 to target multiple genes in the top 20 most enriched pathway. IRF8 targeted 2 pathways, while GBX2 and IKZF1 targeted only 1 pathway. All pathways shown here have an adjusted p-value < 0.007, with the yellow nodes indicating higher p-values and lower p-values indicated by dark red nodes. (D). B Data presented as Tukey box plot. RNA-Seq n=10 autopsy control cortex samples vs. n=12 TSC cortical tubers. Statistical test used: modified t-test.

strong expression of SPI1/PU.1 (Figure 2B, B_1, C). As for microglia, nuclear SPI1/PU.1 expression appeared stronger and the overall number of microglia was higher in FCD IIb and TSC (Figure 2B, C, arrowheads). Of note, SPI1/PU.1 expression could also be found localized in the nucleus of malformed cells and occasionally dysmorphic neurons, confirming its translocation to the nucleus (Figure 2B_2, C_1, C_2, F). We found no SPI1/PU.1 expression in CD3 positive T-lymphocytes (not shown). To further validate our findings from the *in silico* analysis we investigated a separate cohort of TSC cortical tubers and surgically resected FCD IIb tissue and confirmed higher SPI1 expression compared to autoptic control tissue (Figure 2D). Next, to unravel the cell-specific localization of SPI1/PU.1, we performed double-labelling with cell

markers for activated microglia (HLA-DR), astrocytes (GFAP), neurons (NeuN) and mTOR activation (pS6). We found SPI1/PU.1 expression exclusively in microglial nuclei and malformed cells that occasionally co-localized with GFAP in TSC and FCD IIb tissue (Figure 2E-G). Additionally, SPI1/PU.1 in malformed cells co-localized with pS6, indicating mTOR hyperactivation; however, the signal strength of SPI1/PU.1 was heterogeneous in the population of malformed cells (Figure 2H).

Since we observed a strong positive correlation between SPI1 and IRF8 ($\rho = 0.87$, p-value = 1.54×10^{-7}) (Supplementary Figure 2A) and as it has previously been

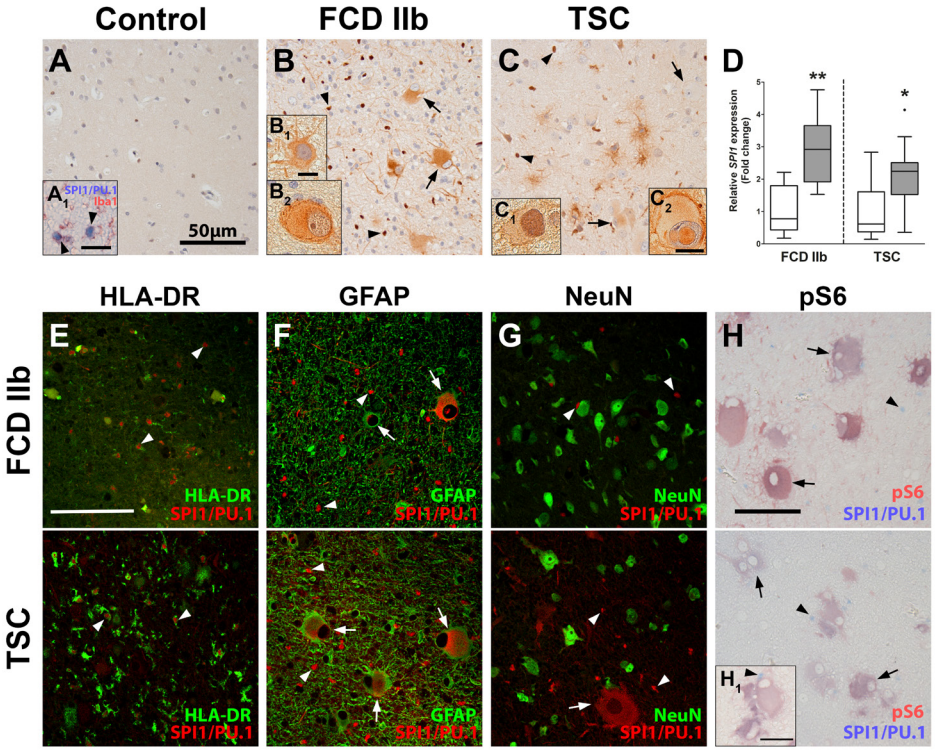

Figure 2: SPI1/PU.1 is highly expressed in malformed cells in TSC and FCD IIb lesions. Autopsy control cortex showed SPI1/PU.1 expression solely in microglia (A, A_1). In TSC and FCD IIb expression of SPI1/PU.1 was found in microglia (arrowheads) but also malformed cells and dysmorphic neurons (arrows) (B, B_1, C). Moreover, SPI1/PU.1 expression could also be found in the nuclei of malformed cells (B_2, C_1, C_2). Analysis of RNA expression in tissue from resected TSC tuber and FCD IIb lesion of an independent cohort showed higher expression of SPI1 compared to control (D). Co-labelling with cell markers HLA-DR, GFAP and NeuN revealed SPI1/PU.1 expression in microglial nuclei (arrowheads) and $GFAP^+NeuN^-$ malformed cells (arrows) in FCD IIb and TSC tissue (E-G). Moreover, malformed cells displayed nuclear SPI1/PU.1 expression (arrows in F). Co-labelling with pS6 showed consistent co-localization with SPI1/PU.1 in malformed cells (H, H_1). Sections A-C were counterstained with hematoxylin. Scale bars: 50 µm in A, E, H, 5 µm in insert B_1 (representative for B_2, C_1), 10 µm in C_2, H_1; arrows = malformed cells, arrowheads = microglia. D Mann-Whitney U-test. Data are expressed relative to expression observed in autopsy controls and displayed as Tukey box plot; * $p<0.05$, ** $p<0.01$. n = 8 autopsy control (for both FCD and TSC control groups) vs. n = 10 TSC and n = 8 FCD IIb samples.

described that SPI1/PU.1 works in unison with Irf8 to regulate the development and activation of microglia (33, 79), we were interested if the same TF axis of SPI1/PU.1 and Irf8 was active in the malformed cells of TSC and FCD IIb. First, we assessed the expression of IRF8 in a cohort of surgically resected FCD IIb tissue and showed that similarly to SPI1, the expression of IRF8 was also higher compared to autoptic control tissue (Supplementary Figure 2B). Next, to assess localisation of the two TFs double-labelling of SPI1/PU.1 and IRF8 was performed in TSC and FCD IIb tissue. IRF8 expression was detected in the nucleus of microglial (arrowheads) and giant and balloon cells (arrows) (Supplementary Figure 2C, D). In malformed cells, IRF8 expression co-localised with SPI1/PU.1 (Supplementary Figure $2C_1$, D_1, D_2). Collectively, these results suggest that the TFs SPI1/PU.1and IRF8 are co-expressed in malformed cells.

SPI1/PU.1 expression in malformed cells is present early in development and precedes seizure development

To assess the effect of age on SPI1 expression, we correlated age with SPI1 expression as assayed by RNA-Seq. While SPI1 was positively correlated (ρ=0.69, p-value = 0.033) with the age of the control cases, it was negatively correlated with the age of patients with TSC cortical tubers (ρ = -0.74, p-value = 0.0064) (Figure 3A, B). This suggests that up-regulation of SPI1 was most prominent in the younger TSC samples. As such, we investigated if SPI1/PU.1 dysregulation represents an early pathogenic mechanism by analysing fetal TSC tissue obtained from autopsy. We found SPI1/PU.1 expression only in very few, sparsely distributed cells with microglial morphology in fetal control tissue (Figure 3C, arrowheads). In comparison, fetal TSC tissue displayed SPI1/PU.1 expression in clusters of malformed cells that could be found in the white matter or adjacent to the developing cortex (Figure 3D). As in postnatal TSC tissue, malformed cells displayed heterogeneous expression patterns of SPI1/PU.1 (Figure $3D_1$).

Spi1 RNA but not protein expression precedes the development of seizures in *Tsc1*$^{GFAP-/-}$ mice

To further investigate the role of SPI1/PU.1 in the transcriptional network of TSC, we employed the *Tsc1*$^{GFAP-/-}$ mouse model which presents with delayed seizure onset, resulting from conditional Tsc1 loss of function in GFAP expressing cells. The delay in seizure onset indicates that other factors additional to the principal mutation and resulting cell autonomous mTOR hyperactivation cause epilepsy, such as alterations in the transcriptional profile over time. Though this model does not recapitulate all the histological features of human TSC, the conditional KO of the *Tsc1* gene in GFAP expressing cells during brain development leads to consistent development of spontaneous recurrent seizures. Moreover, seizure development occurs with a delay of approximately 4-6 weeks after birth, so this model allows analysis of potentially epileptogenic processes due to mTOR activation in the time period

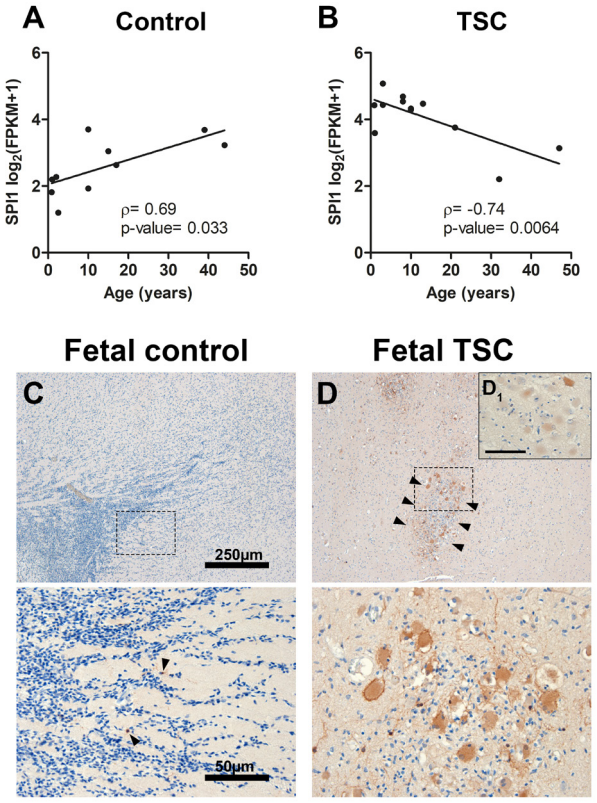

Figure 3: SPI1/PU.1 expression in malformed cells occurs early in TSC development. SPI1 expression displayed a significant positive correlation with age in control samples (A). Contrary, TSC tuber tissue displayed a negative correlation with age samples (Pearson's correlation) (B). Fetal control cortex displayed sparse SPI1/PU.1 expression solely in few microglia (arrowheads in magnified lower panel) (C). Fetal TSC cases revealed strong expression of SPI1/PU.1 in malformed cells that could be found in subcortical clusters (arrowheads, magnified in lower panel) (D). SPI1/PU.1 expression was found to be variable between malformed cells (D_1). Sections C, D were counterstained with hematoxylin. Scale bars: 250 µm in upper panel and 50 µm in C (representative for D), 25 µm in D_1; A, B Spearman's rank correlation test (displayed with Spearman correlation coefficient ρ and exact p-value).

before seizure-onset. Spi1/Pu.1 expression was exclusively detected in microglia in the cortex of control and *Tsc1*$^{GFAP-/-}$ animals (Figure 4A-D). Overall, the number of Spi1/Pu.1 expressing cells between WT and KO was similar in 2-week-old animals, while 2-month-old *Tsc1*$^{GFAP-/-}$ animals displayed higher numbers of Spi1/Pu.1 positive microglia (Figure 4E). Employing in-situ hybridization, Spi1 expression could not be detected in 2-week-old WT animals, but in neurons and glia in 2-month-old WT animals (Figure 4F, H). Relative to WT animals, *Tsc1*$^{GFAP-/-}$ animals displayed higher expression of Spi1 in neurons and glia (Figure 4G, I). Double labelling confirmed co-localization of Spi1 with GFAP, pS6 and Iba-1 (Figure 4I_1, I_2, I_3). Quantification of total RNA expression in *Tsc1*$^{GFAP-/-}$ mice revealed higher expression of Spi1 in the cortex

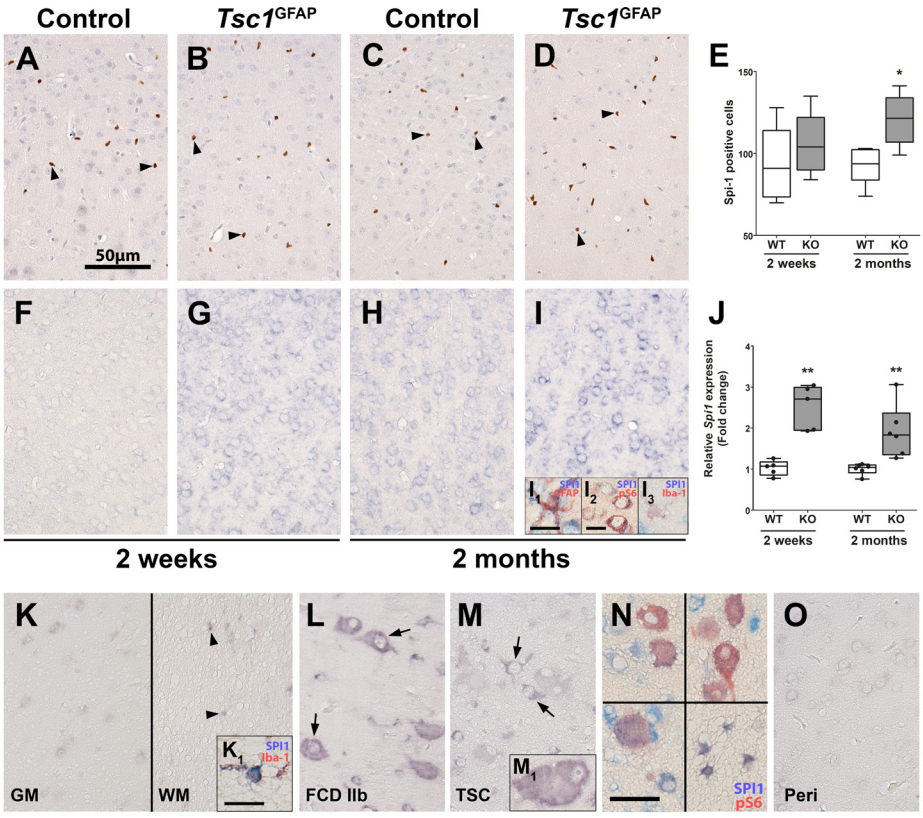

Figure 4: Spi1/Pu.1 RNA expression in the cortex is elevated in *Tsc1*$^{GFAP-/-}$ mice, while protein expression increases with microglial cell number. Antibody staining against Spi1/Pu.1 expressing cells in the cortex of *Tsc1*$^{GFAP-/-}$ mice was not different in 2-week-old animals between WT and KO and restricted to microglia (A, B). In contrast, the number of Spi1/Pu.1 expressing cells was higher in KO animals at 2 months (C, D). Quantification of Spi1/Pu.1 expressing cells in the cortex confirmed higher Spi1/Pu.1 positive cell count in 2-month-old *Tsc1*$^{GFAP-/-}$ animals (E). *In situ* hybridization against Spi1 in the cortex of *Tsc1*$^{GFAP-/-}$ mice showed higher expression of Spi1 at 2-weeks of age in all cell types before seizure development compared to age-matched animals, where expression was absent (F, G). In 2-months old animals Spi1 expression appeared higher in control animals compared to 2-week-old mice (H). In 2-months old animals that suffered from spontaneous recurrent seizures, very strong Spi1 expression could be detected in astrocytes, microglia and pS6-positive neurons (I, I_{1-3}). Quantification of total Spi1 RNA confirmed higher Spi1 RNA expression in *Tsc1*$^{GFAP-/-}$ animals compared to age-matched littermates (J). *In situ* hybridization in human autopsy tissue revealed very weak expression in cortical neurons, and mostly cells with microglial morphology, as confirmed by co-labelling with Iba-1 (K, K_1). SPI1 in FCD IIb lesions and TSC tubers could be found in malformed cells (L, M, M_1). Moreover, SPI1 co-localized with pS6 expression in malformed cells, but also cells with astrocyte morphology (N). Peri-lesional tissue displayed expression similar to autopsy control tissue (O). Sections A-D were counterstained with hematoxylin. Scale bars: 50 µm in A (representative for B-D, F-I, K-M, O), 25 µm in N, 15 µm in I_2, 10 µm in I_1 (representative for I_3) and K_1 (representative for M_1) arrowheads in A = microglia, arrowheads in K = glia, arrows in L, M = malformed cells. E, J Mann-Whitney U-test. Data are expressed relative to expression observed in age-matched wild-type controls and displayed as Tukey box plots; * $p<0.05$, ** $p<0.01$. n = 5 wild-type animals vs. n = 6 *Tsc1*$^{GFAP-/-}$ mice.

of 2-week-old mice prior to development of seizures which persisted to the age of two months when spontaneous recurrent seizures occurred (Figure 4J). In human autopsy control tissue, SPI1 could be detected faintly in grey matter neurons, as well as cells with (micro-)glial morphology in the white matter using *in situ* hybridization (Figure 4K, K_1). In FCD IIb and TSC tissue, we found higher SPI1 expression in dysmorphic neurons and some balloon/giant cells (Figure 4L, M, M_1). Additionally, SPI1 was detected in pS6-positive balloon/giant cells and white matter astrocytes (Figure 4N). In contrast, perilesional tissue displayed faint neuronal expression similar to control (Figure 4O). These findings supported that SPI1 RNA expression is elevated in malformed cells and glia TSC. Moreover, SPI1 expression appeared to be increased consistently in *Tsc1* KO animals, while protein expression was limited to microglial nuclei.

Oxidative stress is evident in TSC tissue and represents a driver for SPI1 transcription *in vitro* in various cells

After we identified SPI1/PU.1 expression to be upregulated in malformed cells and its involvement early in TSC development, we investigated which pathogenic stimuli might drive the expression of SPI1/PU.1. While brain inflammation is a well characterized phenomenon in cortical tubers of TSC patients, we also found expression of the pro-oxidant enzyme iNOS in malformed cells and activation of anti-oxidant gene expression in whole TSC tissue, indicative of oxidative stress (Figure 5A-C). Here, we detected some cells displaying co-expression of SPI/PU.1 and iNOS, but also iNOS-positive cells surrounded by SPI/PU.1-expressing cells (Figure 5A_1, A_2, B_1). These cells did not present with typical dysmorphic neuron or balloon/giant cell morphology, but rather presented with dysplastic, process-rich, astrocytic morphology. We used human fetal astrocytes to further characterize SPI1 expression in response to TSC-relevant stimuli. Since we found a strong correlation between IL-1β and SPI1 ($\rho = 0.817$) in the sequencing dataset we investigated if IL-1β can induce SPI1/PU.1. Therefore, we stimulated fetal astrocytes with IL-1β to study if pro-inflammatory stimuli regulate SPI1; however, we could not detect any differences in SPI1 expression (Figure 5D). On the other hand, stimulation of fetal astrocytes with H_2O_2 led to a time-dependent upregulation of SPI1, similar to TSC derived astrocytes (Figure 5E). Surprisingly, SPI1 expression could even be induced in the neuroblastoma cell line SH-SY5Y upon oxidative stress in a concentration-dependent manner (Figure 5F). Furthermore, to test if mTOR hyperactivation *per se* drives SPI1 expression, we analysed SPI1 expression in astrocytes derived from TSC tubers. Additionally, we stimulated TSC astrocytes with H_2O_2 only or in combination with the mTOR inhibitor rapamycin to untangle if oxidative stress and/or mTOR hyperactivation are involved in SPI1 expression. Interestingly, we found a strong induction of SPI1 by H_2O_2 in TSC astrocytes, which could not be blocked by rapamycin treatment (Figure 5G). Importantly, SPI1 in one of three unstimulated TSC-astrocyte cultures was below detection level. Collectively, these results indicate that oxidative

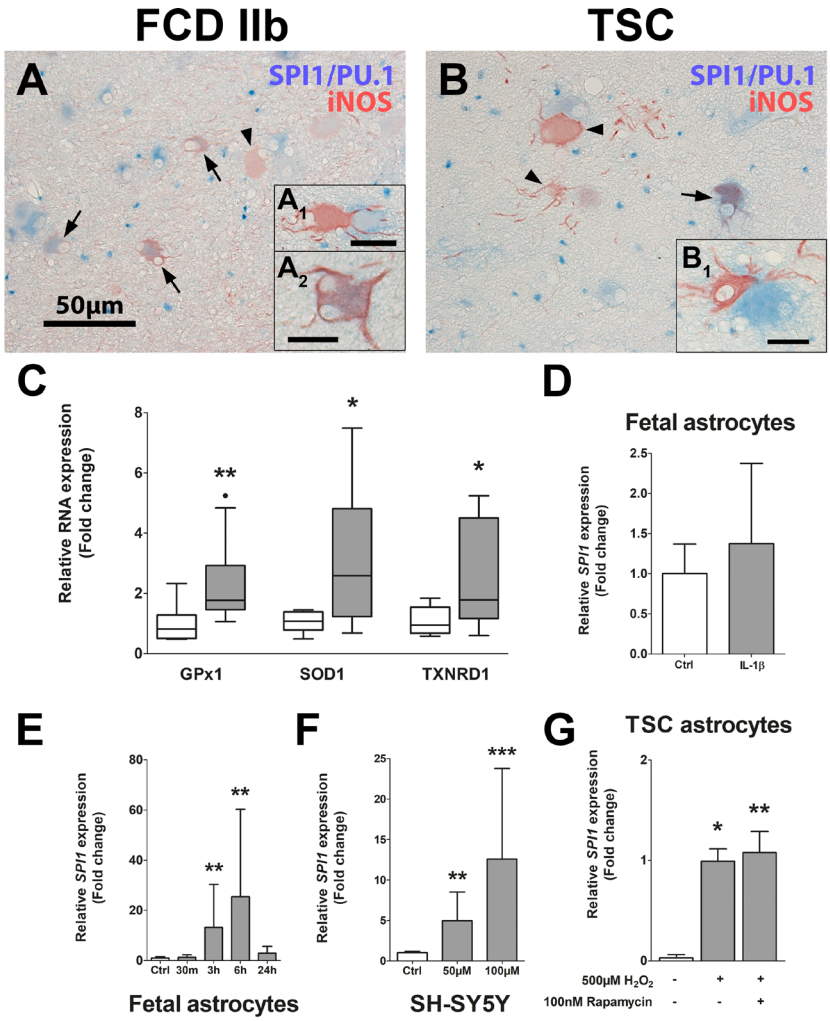

Figure 5: Oxidative stress is present in malformed cells in TSC cortical tubers and stimulates SPI1 expression *in vitro*. Expression of iNOS could be detected exclusively in malformed cells in FCD IIb and TSC tissue. Co-localization of SPI/PU.1 and iNOS was found in some malformed cells (arrows in A, B and A_2). Moreover, iNOS expression was often found in cells that were in close proximity to SPI1/PU.1 expressing cells (A_1, B_1) that wrapped around each other (A, B). Analysis of the OS markers GPx1, SOD1 and TXNRD1 showed higher expression in TSC tissue compared to control (C). Human fetal astrocytes did not display higher SPI1 expression when exposed to IL-1β, but H_2O_2 in a time-dependent manner (D, E). SH-SY5Y neuroblastoma cells exposed to H_2O_2 displayed SPI1 induction, similar to astrocytes (F). *In vitro*, TSC-derived astrocytes displayed higher expression of SPI1 when exposed to H_2O_2, which was independent of mTOR inhibition via rapamycin (G). Scale bars: 50 µm in A, 25 µm in A_1, 20 µm in B_1, 10 µm in A_2, arrowheads = iNOS single positive cells, arrows = co-localized cells. C, D Mann Whitney U-test. E-G Kruskal Wallis test with Dunn's *post hoc*. C Data are expressed relative to expression in autopsy control and displayed as Tukey box plot. D-G Data are expressed as bar graphs with SD; * p<0.05, ** p<0.01, ***p<0.001. C n = 8 autopsy control vs. n = 10 TSC samples. D-G n = 3 independent cultures in duplicates.

stress strongly induces SPI1 RNA expression in a multitude of cell types, and that this stimulation on the RNA level is independent of cell-autonomous mTOR hyperactivity in TSC-derived cells.

Discussion

In this study, we investigated the transcriptional regulation of the TSC tuber environment and identified the transcription factor SPI1/PU.1 as pathogenic transcriptional regulator in TSC and could confirm its dysregulation in the related pathology FCD IIb. We found strong correlation with a variety of pro-inflammatory mediators, making SPI1/PU.1 a candidate driver of brain inflammation. SPI1/PU.1 expression was concentrated in malformed cells in lesions and its upregulation could be seen during fetal development. Moreover, we found SPI1/PU.1 expression in dysmorphic cells with mTOR activation and in glia in TSC tubers, FCD IIb lesions and prenatal TSC brain tissue, which concur with higher RNA expression in *Tsc1*$^{GFAP-/-}$ mice. Moreover, we found that oxidative stress potently drives transcriptional activation of SPI1 in a variety of cells *in vitro*, including TSC-derived astrocytes. While we identified elevated SPI1 RNA expression, likely promoted via oxidative stress, SPI1/PU.1 protein translation appears to critically rely on translation defects specific to mTOR activation in malformed cells TSC and FCD IIb lesions.

Identification of TFs that are major regulators of the underlying pathogenesis of TSC could aid in the development of new therapeutic tools that could modify the disease course in TSC and other mTORopathies. Here, we employed various unbiased *in silico* approaches across previously produced RNA-Seq datasets to identify transcriptional regulators that potentially influence the differential expressions pattern seen in TSC. We extracted four upregulated TFs from the data: SPI1/PU.1, IRF8, GBX2 and IKZF1. After an enrichment analysis of the upregulated genes for TF targets we did not detect significant enrichment of upregulated genes for GBX2 and IKZF1, thus we did not focus further on these TFs. However, since little is known about the function of these TFs, the data available on the reference repositories employed for gene enrichment analysis is limited, influencing the outcome of this analysis. Nevertheless, these TFs might serve important modulatory functions in TSC tubers. Moreover, we aimed to identify novel drivers of gene expression in TSC and not repressors. For instance, GBX2 was shown to have important roles as a transcriptional repressor in telencephalic development in zebrafish (45, 74) and specifically development of forebrain GABAergic neurons in mice (54). On the other hand, IKZF1 is a transcriptional regulator of erythropoiesis (73) and, in the brain, was implicated in transcriptional alterations in neurodegeneration, neuronal differentiation and functions of the endocrine system (1, 21, 38, 66). Interestingly, syndromes caused by deletions of IKZF1 present with intellectual disability (30). Taken together, upregulation of GBX2 and IKZF1 could still reflect important changes in the aberrant brain development

and syndromes of TSC by mild modulation of neural development genes below the cut-off p-value or by acting as repressors. Furthermore, it is important to consider the contribution of the altered cellular composition of the tuber, as GBX2 upregulation could also reflect lymphocyte infiltration, a feature commonly observed in TSC tubers (7, 48). While other TFs previously implicated in TSC, such as tp53 and NF-κB, were not up-regulated, we still analysed gene enrichment for these TFs (22, 24, 37, 40). We could retrieve data only for RelA for which a significant enrichment value was calculated. Since this transcription factor is involved in the activation of a number of pro-inflammatory genes, its enrichment in TSC tuber was anticipated from previous studies (2, 40). In *tsc2*$^{-/-}$ zebrafish, we detected up-regulation of Spi1b, Ikzf1, tp53 and Rel, as well as RelB down-regulation, while gene enrichment was computed for Spi1b, Irf8 and RelA. Because we detected up-regulation and enrichment of up-regulated genes for SPI1 and its homologue in both human and zebrafish data, we focused our attention on SPI1 as transcriptional driver. We did not focus on NF-κB TFs since these were already previously characterized in TSC (24, 40).

SPI1/PU.1 is a transcriptional activator, known to regulate the expression of hundreds of genes by binding to a purine-rich sequence, known as PU-box that is found adjacent to the promoter region of its target genes (35, 49, 55). More specifically, SPI1/PU.1 is integral for the maturation of microglia, lymphocytes, and the majority of myeloid cell lines. As such, SPI1/PU.1 is critical to the maturation and regulation of the immune system and brain inflammation, two processes that are pathogenic hallmarks of TSC (27, 51, 67). Furthermore, SPI1/PU.1 has been instigated in leukemia, Alzheimer's disease and, notably in the context of epileptogenic pathologies, in the chronic transcriptional changes that result from experimental traumatic brain injury (TBI) in rats (39, 52, 59). In our data-set, SPI1/PU.1 enriched for genes involved in Toll-like receptor (TLR) signalling, complement activation and cytokine signalling, all of which support the pro-inflammatory environment in TSC and SPI1/PU.1 as potential activator of these processes. Importantly, these processes were shown to be activated in malformed cells in TSC tubers previously (6, 7, 81). Since innate and adaptive immune cells play a role in these inflammatory processes, we wondered if peripheral immune cells and microglia, malformed cells with cell-autonomous mTOR activation or all cell types contribute to the inflammatory environment in TSC tubers. Since SPI1/PU.1 in microglia is essential for viability and phenotypic differentiation, its expression in microglia was expected (33, 61). While more activated microglia can be found in tubers, we also localized SPI1/PU.1 expression to malformed cells in TSC and FCD IIb, respectively. Moreover, we also identified IRF8 and its target genes to be upregulated in cortical tubers, a factor that is essential for microglia development and activation (33, 79). This suggests that increased microglial numbers and their activation contribute to the higher expression of SPI1/PU.1 and its target genes, a feature previously demonstrated in TSC tubers (7, 8). However, we also detected expression of these factors in malformed cells. It is noteworthy, that despite SPI1/

PU.1 expression in microglia usually being localized strictly to the nucleus, in malformed cells we detected frequently cytoplasmic expression. One reason could be a disturbed redox balance due to oxidative stress, preventing regulated nuclear translocation of SPI1/PU.1 in malformed cells as shown by a previous study (41). Nevertheless, we still detected malformed cells with nuclear expression, thus potentially active SPI1/PU.1.

Interestingly, SPI1/PU.1 expression is already elevated in fetal TSC brain tissue in malformed cells, before terminal differentiation of microglial cells at approximately gestational week (GW) 35 (20, 25, 50, 72). The fetal TSC cases included in our study were GW 27 and GW 32 (GW32 in the representative picture), respectively. This indicates that malformed cells already display SPI1/PU.1 expression before brain-wide infiltration, differentiation and potentially activation of microglia, enabling pro-inflammatory transcriptional programs to be activated in malformed cells already during development. In support of this, conditional KO of Tsc1 in *Tsc1*$^{GFAP-/-}$ also induced an early transcription of Spi1. Interestingly, we found wide-spread expression of Spi1 in the cortex of *Tsc1*$^{GFAP-/-}$ mice, in astrocytes, neurons and microglia. Contrary, Spi1/Pu.1 protein expression could only be localized to microglial nuclei.
SPI1/PU.1 is a TF solely restricted to microglia and infiltrating immune cells in the healthy brain and PU.1 is frequently used as microglia/monocyte marker in the brain. Thus, we anticipated that mTOR hyperactivation in malformed cells would be the aberrant driving force for SPI1/PU.1 expression in malformed cells. Remarkably, we found oxidative stress to strongly induce SPI1 expression in a time- and concentration-dependent manner in astrocytes and the SH-SY5Y neuroblastoma cell line. Most importantly, inhibition with rapamycin in TSC-derived astrocytes had no effect on increased SPI1 expression, suggesting mTOR independent activation of SPI1 RNA expression. While we cannot rule out secondary inflammatory signalling in response to oxidative stress (65), direct receptor-mediated pro-inflammatory stimulation with IL-1β, that normally induces a robust inflammatory response in fetal astrocytes (69, 70), did not alter SPI1/PU.1 expression. Moreover, we detected up-regulation of antioxidant genes, an indicator of elevated oxidative stress, in tuber tissue in agreement with previous studies (2, 80). Importantly, expression of oxidative stress response genes characterized in previous studies coincides with SPI1 expression in fetal TSC and in the brain of *Tsc1*$^{GFAP-/-}$ mice (80). Hence, we conclude that oxidative stress is a driver of SPI1/PU.1 RNA expression, which is supported by previous studies showing that TFs induced by oxidative stress can stimulate SPI1 expression (63). Moreover, oxidative stress is a potent activation signal for a multitude of TFs and could lead to their translocation and transcriptional activation of SPI1 transcription (26).

While we detected robust RNA expression across *in vitro* and *in vivo* models, we did not detect Spi1/Pu.1 protein expression in cells other than microglia in

Tsc1$^{GFAP-/-}$ mice. However, while Spi1 was elevated already at two weeks of age, the number of microglia was not increased, only after the development of seizures at 2 months, in agreement with previous reports about this model (78). This suggests that oxidative stress due to mTOR activation stimulates Spi1 mRNA expression in a variety of cells, but other post-transcriptional regulatory mechanisms inhibit Spi1/Pu.1 translation. While initial SPI1 RNA expression appears to be driven by oxidative stress, translational dysregulation of SPI1 mRNA might require a trigger present in cells with aberrant cell-autonomous mTOR activation, such as malformed cells. The lack of protein translation suggests that Spi1/Pu.1 in *Tsc1*$^{GFAP-/-}$ mice does not play the same pro-inflammatory role as in TSC tubers from patients. However, this model and the zebrafish model confirm that an environment of mTOR hyperactivation promotes oxidative stress mediated Spi1 expression. Moreover, microglia-specific upregulation of PU.1 in response to oxidative stress could certainly exert pro-inflammatory effects secondary to mTOR hyperactivation.

We hypothesize that mTOR activation in malformed cells predisposes specifically this cell population to SPI1 translation due to promotion of protein synthesis and suppression of protein catabolism by mTOR complex 1 (56). Since replication of malformed cells and tubers in TSC models is still lacking, it is currently impossible to model this particular aspect. Interestingly, the precursor of malformed cells is hypothesized to be a human-specific radial glia cell population, that could only be replicated in human-derived organoid models (47). To ultimately verify our hypothesis, ChIP-Seq experiments should be performed on malformed cells of tuber tissue or derived from TSC-derived organoids to confirm binding of SPI1/PU.1 to putative transcriptional targets. While it was shown that it is possible to isolate and culture malformed cells *in vitro* (75), only few cells can be isolated and large-scale ChIP-Seq experiments are therefore not feasible. Moreover, replicating malformed cells and their characteristic features *in vitro* remains difficult to date. While we analysed SPI1 expression in TSC-derived astrocytes, these cells do not recapitulate all the features of dysmorphic neurons and giant/balloon cells, the cells displaying the strongest SPI1/PU.1 expression. Moreover, it remains questionable if the tuber microenvironment is properly replicated *in vitro* and we assume this factor also plays an essential part in mediating aberrant protein translation in malformed cells. While we acknowledge the contribution of microglia and other leukocytes to SPI1/PU.1 up-regulation in TSC tubers, we conclude that SPI1/PU.1 in malformed cells with intrinsic mTOR activation drives the execution of immunogenic transcriptional programs normally only present in microglia, promoting the expression of pro-inflammatory factors such as complement or cytokines. Thus, by specifically targeting this transcription factor it could be possible to dampen inflammation mediated by these cells in TSC and other mTORopathies like FCD IIb.

Declarations

All procedures performed in studies involving human participants were in accordance

with the Amsterdam UMC Research Code provided by the Medical Ethics Committee and with the 1964 Helsinki declaration and its later amendments or comparable ethical standards. All procedures performed in studies involving animals were in accordance with the ethical standards of the Washington University Animal Welfare committee.

Consent for publication

All authors read and agreed with the contents of this paper.

Availability of data and materials

The original RNA sequencing data utilized for the identification of the transcription

factors can be found in the primary publication (https://doi.org/10.1038/s41598-017-06145-8). The datasets generated and/or analysed during the current study are available in the European Genome-phenome Archive, using accession codes for primary (EGAS00001002485) and secondary (GSE67835) RNA sequencing data.

Conflict of interest

The authors declare that they have no conflict of interest.

Funding

The research leading to these results has received funding from the European Union's Seventh Framework Programme (FP7/2007-2013) under grant agreement no. 602391 (EPISTOP; EA), the Dutch Epilepsy Foundation, project number 16-05 and 20-11 (EAvV), project number 10-02 (AM), the European Union's Horizon 2020 Research and Innovation Programme under the Marie Sklodowska-Curie grant agreement no. 642881 (ECMED; AK, EA), no. 722053 (EU-GliaPhD; TSZ, EA) and the United States National Institutes of Health R01 NS056872 (MW).

Author's contributions

TSZ, AK, SZ, FJTZ, and JDM performed the experiments, data collection and analysis. FEJ, AM, NRR, MW, EAvV, JDM and EA helped with the selection and collection of brain tissues and clinical data. JDM, EAvV and EA conceived the study and participated in its design and coordination. TSZ, JDM, EAvV and EA drafted and prepared the manuscript. All authors read, revised, and approved the final manuscript.

Acknowledgments

Not applicable

References

1. Agoston DV, Szemes M, Dobi A, Palkovits M, Georgopoulos K, Gyorgy A, Ring MA (2007) Ikaros is expressed in developing striatal neurons and involved in enkephalinergic differentiation. J Neurochem.102(6):1805-16.
2. Arena A, Zimmer TS, van Scheppingen J, Korotkov A, Anink JJ, Muhlebner A, Jansen FE, van Hecke W, Spliet WG, van Rijen PC, Vezzani A, Baayen JC, Idema S, Iyer AM, Perluigi M, Mills JD, van Vliet EA, Aronica E (2019) Oxidative stress and inflammation in a spectrum of epileptogenic cortical malformations: molecular insights into their interdependence. Brain Pathol.29(3):351-65.
3. Aronica E, Crino PB (2014) Epilepsy related to developmental tumors and malformations of cortical development. Neurotherapeutics.11(2):251-68.
4. Baldassari S, Ribierre T, Marsan E, Adle-Biassette H, Ferrand-Sorbets S, Bulteau C, Dorison N, Fohlen M, Polivka M, Weckhuysen S, Dorfmuller G, Chipaux M, Baulac S (2019) Dissecting the genetic basis of focal cortical dysplasia: a large cohort study. Acta Neuropathol.138(6):885-900.
5. Blumcke I, Thom M, Aronica E, Armstrong DD, Vinters HV, Palmini A, Jacques TS, Avanzini G, Barkovich AJ, Battaglia G, Becker A, Cepeda C, Cendes F, Colombo N, Crino P, Cross JH, Delalande O, Dubeau F, Duncan J, Guerrini R, Kahane P, Mathern G, Najm I, Ozkara C, Raybaud C, Represa A, Roper SN, Salamon N, Schulze-Bonhage A, Tassi L, Vezzani A, Spreafico R (2011) The clinicopathologic spectrum of focal cortical dysplasias: a consensus classification proposed by an ad hoc Task Force of the ILAE Diagnostic Methods Commission. Epilepsia.52(1):158-74.
6. Boer K, Crino PB, Gorter JA, Nellist M, Jansen FE, Spliet WG, van Rijen PC, Wittink FR, Breit TM, Troost D, Wadman WJ, Aronica E (2010) Gene expression analysis of tuberous sclerosis complex cortical tubers reveals increased expression of adhesion and inflammatory factors. Brain Pathol.20(4):704-19.
7. Boer K, Jansen F, Nellist M, Redeker S, van den Ouweland AM, Spliet WG, van Nieuwenhuizen O, Troost D, Crino PB, Aronica E (2008) Inflammatory processes in cortical tubers and subependymal giant cell tumors of tuberous sclerosis complex. Epilepsy Res.78(1):7-21.
8. Boer K, Troost D, Jansen F, Nellist M, van den Ouweland AM, Geurts JJ, Spliet WG, Crino P, Aronica E (2008) Clinicopathological and immunohistochemical findings in an autopsy case of tuberous sclerosis complex. Neuropathology.28(6):577-90.
9. Broekaart DWM, van Scheppingen J, Anink JJ, Wierts L, van Het Hof B, Jansen FE, Spliet WG, van Rijen PC, Kamphuis WW, de Vries HE, Aronica E, van Vliet EA (2020) Increased matrix metalloproteinases expression in tuberous sclerosis complex: modulation by microRNA 146a and 147b in vitro. Neuropathol Appl Neurobiol.46(2):142-59.
10. Crino PB (2010) The pathophysiology of tuberous sclerosis complex. Epilepsia.51 Suppl 1:27-9.
11. Crino PB (2013) Evolving neurobiology of tuberous sclerosis complex. Acta Neuropathol.125(3):317-32.
12. Crino PB, Aronica E, Baltuch G, Nathanson KL (2010) Biallelic TSC gene inactivation in tuberous sclerosis complex. Neurology.74(21):1716-23.
13. Curatolo P, Bombardieri R, Jozwiak S (2008) Tuberous sclerosis. Lancet.372(9639):657-68.
14. Curatolo P, Moavero R, de Vries PJ (2015) Neurological and neuropsychiatric aspects of tuberous sclerosis complex. Lancet Neurol.14(7):733-45.
15. Di Nardo A, Kramvis I, Cho N, Sadowski A, Meikle L, Kwiatkowski DJ, Sahin M (2009) Tuberous sclerosis complex activity is required to control neuronal stress responses in an mTOR-dependent manner. J Neurosci.29(18):5926-37.
16. Dombkowski AA, Batista CE, Cukovic D, Carruthers NJ, Ranganathan R, Shukla U, Stemmer PM, Chugani HT, Chugani DC (2016) Cortical Tubers: Windows into Dysregulation of Epilepsy Risk and Synaptic Signaling Genes by MicroRNAs. Cereb Cortex.26(3):1059-71.
17. Durinck S, Moreau Y, Kasprzyk A, Davis S, De Moor B, Brazma A, Huber W (2005) BioMart and Bioconductor: a powerful link between biological databases and microarray data analysis. Bioinformatics.21(16):3439-40.
18. Durinck S, Spellman PT, Birney E, Huber W (2009) Mapping identifiers for the integration of genomic datasets with the R/Bioconductor package biomaRt. Nat Protoc.4(8):1184-91.
19. Erbayat-Altay E, Zeng LH, Xu L, Gutmann DH, Wong M (2007) The natural history and treatment of epilepsy in a murine model of tuberous sclerosis. Epilepsia.48(8):1470-6.
20. Esiri MM, al Izzi MS, Reading MC (1991) Macrophages, microglial cells, and HLA-DR antigens in fetal and infant brain. J Clin Pathol.44(2):102-6.

21. Ezzat S, Mader R, Yu S, Ning T, Poussier P, Asa SL (2005) Ikaros integrates endocrine and immune system development. J Clin Invest.115(4):1021-9.
22. Feng Z, Zhang H, Levine AJ, Jin S (2005) The coordinate regulation of the p53 and mTOR pathways in cells. Proc Natl Acad Sci U S A.102(23):8204-9.
23. Fuso A, Iyer AM, van Scheppingen J, Maccarrone M, Scholl T, Hainfellner JA, Feucht M, Jansen FE, Spliet WG, Krsek P, Zamecnik J, Muhlebner A, Aronica E (2016) Promoter-Specific Hypomethylation Correlates with IL-1beta Overexpression in Tuberous Sclerosis Complex (TSC). J Mol Neurosci.59(4):464-70.
24. Ghosh S, Tergaonkar V, Rothlin CV, Correa RG, Bottero V, Bist P, Verma IM, Hunter T (2006) Essential role of tuberous sclerosis genes TSC1 and TSC2 in NF-kappaB activation and cell survival. Cancer Cell.10(3):215-26.
25. Ginhoux F, Prinz M (2015) Origin of microglia: current concepts and past controversies. Cold Spring Harb Perspect Biol.7(8):a020537.
26. Go YM, Jones DP (2010) Redox control systems in the nucleus: mechanisms and functions. Antioxid Redox Signal.13(4):489-509.
27. Huang KL, Marcora E, Pimenova AA, Di Narzo AF, Kapoor M, Jin SC, Harari O, Bertelsen S, Fairfax BP, Czajkowski J, Chouraki V, Grenier-Boley B, Bellenguez C, Deming Y, McKenzie A, Raj T, Renton AE, Budde J, Smith A, Fitzpatrick A, Bis JC, DeStefano A, Adams HHH, Ikram MA, van der Lee S, Del-Aguila JL, Fernandez MV, Ibanez L, International Genomics of Alzheimer's P, Alzheimer's Disease Neuroimaging I, Sims R, Escott-Price V, Mayeux R, Haines JL, Farrer LA, Pericak-Vance MA, Lambert JC, van Duijn C, Launer L, Seshadri S, Williams J, Amouyel P, Schellenberg GD, Zhang B, Borecki I, Kauwe JSK, Cruchaga C, Hao K, Goate AM (2017) A common haplotype lowers PU.1 expression in myeloid cells and delays onset of Alzheimer's disease. Nat Neurosci.20(8):1052-61.
28. Iffland PH, 2nd, Crino PB (2017) Focal Cortical Dysplasia: Gene Mutations, Cell Signaling, and Therapeutic Implications. Annu Rev Pathol.12:547-71.
29. Jansen FE, van Huffelen AC, Algra A, van Nieuwenhuizen O (2007) Epilepsy surgery in tuberous sclerosis: a systematic review. Epilepsia.48(8):1477-84.
30. Jarviaho T, Zachariadis V, Tesi B, Chiang S, Bryceson YT, Mottonen M, Niinimaki R, Bang B, Rahikkala E, Taylan F, Uusimaa J, Harila-Saari A, Nordgren A (2019) Microdeletion of 7p12.1p13, including IKZF1, causes intellectual impairment, overgrowth, and susceptibility to leukaemia. Br J Haematol.185(2):354-7.
31. Jassal B, Matthews L, Viteri G, Gong C, Lorente P, Fabregat A, Sidiropoulos K, Cook J, Gillespie M, Haw R, Loney F, May B, Milacic M, Rothfels K, Sevilla C, Shamovsky V, Shorser S, Varusai T, Weiser J, Wu G, Stein L, Hermjakob H, D'Eustachio P (2020) The reactome pathway knowledgebase. Nucleic Acids Res.48(D1):D498-D503.
32. Kannan L, Vogrin S, Bailey C, Maixner W, Harvey AS (2016) Centre of epileptogenic tubers generate and propagate seizures in tuberous sclerosis. Brain.139(Pt 10):2653-67.
33. Kierdorf K, Erny D, Goldmann T, Sander V, Schulz C, Perdiguero EG, Wieghofer P, Heinrich A, Riemke P, Holscher C, Muller DN, Luckow B, Brocker T, Debowski K, Fritz G, Opdenakker G, Diefenbach A, Biber K, Heikenwalder M, Geissmann F, Rosenbauer F, Prinz M (2013) Microglia emerge from erythromyeloid precursors via Pu.1- and Irf8-dependent pathways. Nat Neurosci.16(3):273-80.
34. Kloss S, Pieper T, Pannek H, Holthausen H, Tuxhorn I (2002) Epilepsy surgery in children with focal cortical dysplasia (FCD): results of long-term seizure outcome. Neuropediatrics.33(1):21-6.
35. Kodandapani R, Pio F, Ni CZ, Piccialli G, Klemsz M, McKercher S, Maki RA, Ely KR (1996) A new pattern for helix-turn-helix recognition revealed by the PU.1 ETS-domain-DNA complex. Nature.380(6573):456-60.
36. Lachmann A, Xu H, Krishnan J, Berger SI, Mazloom AR, Ma'ayan A (2010) ChEA: transcription factor regulation inferred from integrating genome-wide ChIP-X experiments. Bioinformatics.26(19):2438-44.
37. Lee CH, Inoki K, Karbowniczek M, Petroulakis E, Sonenberg N, Henske EP, Guan KL (2007) Constitutive mTOR activation in TSC mutants sensitizes cells to energy starvation and genomic damage via p53. EMBO J.26(23):4812-23.
38. Li MD, Burns TC, Morgan AA, Khatri P (2014) Integrated multi-cohort transcriptional meta-analysis of neurodegenerative diseases. Acta Neuropathol Commun.2:93.
39. Lipponen A, El-Osta A, Kaspi A, Ziemann M, Khurana I, Kn H, Navarro-Ferrandis V, Puhakka N, Paananen J, Pitkanen A (2018) Transcription factors Tp73, Cebpd, Pax6, and Spi1 rather than DNA methylation regulate chronic transcriptomics changes after experimental traumatic brain injury. Acta Neuropathol Commun.6(1):17.
40. Maldonado M, Baybis M, Newman D, Kolson DL, Chen W, McKhann G, 2nd, Gutmann DH, Crino PB (2003)

Expression of ICAM-1, TNF-alpha, NF kappa B, and MAP kinase in tubers of the tuberous sclerosis complex. Neurobiol Dis.14(2):279-90.

41. Mehta AJ, Joshi PC, Fan X, Brown LA, Ritzenthaler JD, Roman J, Guidot DM (2011) Zinc supplementation restores PU.1 and Nrf2 nuclear binding in alveolar macrophages and improves redox balance and bacterial clearance in the lungs of alcohol-fed rats. Alcohol Clin Exp Res.35(8):1519-28.

42. Mills JD, Iyer AM, van Scheppingen J, Bongaarts A, Anink JJ, Janssen B, Zimmer TS, Spliet WG, van Rijen PC, Jansen FE, Feucht M, Hainfellner JA, Krsek P, Zamecnik J, Kotulska K, Jozwiak S, Jansen A, Lagae L, Curatolo P, Kwiatkowski DJ, Pasterkamp RJ, Senthilkumar K, von Oerthel L, Hoekman MF, Gorter JA, Crino PB, Muhlebner A, Scicluna BP, Aronica E (2017) Coding and small non-coding transcriptional landscape of tuberous sclerosis complex cortical tubers: implications for pathophysiology and treatment. Sci Rep.7(1):8089.

43. Muhlebner A, Bongaarts A, Sarnat HB, Scholl T, Aronica E (2019) New insights into a spectrum of developmental malformations related to mTOR dysregulations: challenges and perspectives. J Anat.235(3):521-42.

44. Najm IM, Sarnat HB, Blumcke I (2018) Review: The international consensus classification of Focal Cortical Dysplasia- a critical update 2018. Neuropathol Appl Neurobiol.44(1):18-31.

45. Nakayama Y, Kikuta H, Kanai M, Yoshikawa K, Kawamura A, Kobayashi K, Wang Z, Khan A, Kawakami K, Yamasu K (2013) Gbx2 functions as a transcriptional repressor to regulate the specification and morphogenesis of the mid-hindbrain junction in a dosage- and stage-dependent manner. Mech Dev.130(11-12):532-52.

46. Pauletti A, Terrone G, Shekh-Ahmad T, Salamone A, Ravizza T, Rizzi M, Pastore A, Pascente R, Liang LP, Villa BR, Balosso S, Abramov AY, van Vliet EA, Del Giudice E, Aronica E, Patel M, Walker MC, Vezzani A (2019) Targeting oxidative stress improves disease outcomes in a rat model of acquired epilepsy. Brain.142(7):e39.

47. Pollen AA, Bhaduri A, Andrews MG, Nowakowski TJ, Meyerson OS, Mostajo-Radji MA, Di Lullo E, Alvarado B, Bedolli M, Dougherty ML, Fiddes IT, Kronenberg ZN, Shuga J, Leyrat AA, West JA, Bershteyn M, Lowe CB, Pavlovic BJ, Salama SR, Haussler D, Eichler EE, Kriegstein AR (2019) Establishing Cerebral Organoids as Models of Human-Specific Brain Evolution. Cell.176(4):743-56 e17.

48. Prabowo AS, Anink JJ, Lammens M, Nellist M, van den Ouweland AM, Adle-Biassette H, Sarnat HB, Flores-Sarnat L, Crino PB, Aronica E (2013) Fetal brain lesions in tuberous sclerosis complex: TORC1 activation and inflammation. Brain Pathol.23(1):45-59.

49. Ray-Gallet D, Mao C, Tavitian A, Moreau-Gachelin F (1995) DNA binding specificities of Spi-1/PU.1 and Spi-B transcription factors and identification of a Spi-1/Spi-B binding site in the c-fes/c-fps promoter. Oncogene.11(2):303-13.

50. Rezaie P, Dean A, Male D, Ulfig N (2005) Microglia in the cerebral wall of the human telencephalon at second trimester. Cereb Cortex.15(7):938-49.

51. Rimmele P, Esposito M, Delestre L, Guervilly JH, Ridinger-Saison M, Despras E, Moreau-Gachelin F, Rosselli F, Guillouf C (2017) The Spi1/PU.1 transcription factor accelerates replication fork progression by increasing PP1 phosphatase in leukemia. Oncotarget.8(23):37104-14.

52. Rustenhoven J, Smith AM, Smyth LC, Jansson D, Scotter EL, Swanson MEV, Aalderink M, Coppieters N, Narayan P, Handley R, Overall C, Park TIH, Schweder P, Heppner P, Curtis MA, Faull RLM, Dragunow M (2018) PU.1 regulates Alzheimer's disease-associated genes in primary human microglia. Mol Neurodegener.13(1):44.

53. Samueli S, Abraham K, Dressler A, Groeppel G, Jonak C, Muehlebner A, Prayer D, Reitner A, Feucht M, Padiatrisches TSCZW (2015) Tuberous Sclerosis Complex: new criteria for diagnostic work-up and management. Wien Klin Wochenschr.127(15-16):619-30.

54. Sandberg M, Flandin P, Silberberg S, Su-Feher L, Price JD, Hu JS, Kim C, Visel A, Nord AS, Rubenstein JLR (2016) Transcriptional Networks Controlled by NKX2-1 in the Development of Forebrain GABAergic Neurons. Neuron.91(6):1260-75.

55. Satoh J, Asahina N, Kitano S, Kino Y (2014) A Comprehensive Profile of ChIP-Seq-Based PU.1/Spi1 Target Genes in Microglia. Gene Regul Syst Bio.8:127-39.

56. Saxton RA, Sabatini DM (2017) mTOR Signaling in Growth, Metabolism, and Disease. Cell.168(6):960-76.

57. Scheldeman C, Mills JD, Siekierska A, Serra I, Copmans D, Iyer AM, Whalley BJ, Maes J, Jansen AC, Lagae L, Aronica E, de Witte PAM (2017) mTOR-related neuropathology in mutant tsc2 zebrafish: Phenotypic, transcriptomic and pharmacological analysis. Neurobiol Dis.108:225-37.

58. Schmidt EV, Ravitz MJ, Chen L, Lynch M (2009) Growth controls connect: interactions between c-myc and

the tuberous sclerosis complex-mTOR pathway. Cell Cycle.8(9):1344-51.
59. Seki M, Kimura S, Isobe T, Yoshida K, Ueno H, Nakajima-Takagi Y, Wang C, Lin L, Kon A, Suzuki H, Shiozawa Y, Kataoka K, Fujii Y, Shiraishi Y, Chiba K, Tanaka H, Shimamura T, Masuda K, Kawamoto H, Ohki K, Kato M, Arakawa Y, Koh K, Hanada R, Moritake H, Akiyama M, Kobayashi R, Deguchi T, Hashii Y, Imamura T, Sato A, Kiyokawa N, Oka A, Hayashi Y, Takagi M, Manabe A, Ohara A, Horibe K, Sanada M, Iwama A, Mano H, Miyano S, Ogawa S, Takita J (2017) Recurrent SPI1 (PU.1) fusions in high-risk pediatric T cell acute lymphoblastic leukemia. Nat Genet.49(8):1274-81.
60. Shekh-Ahmad T, Eckel R, Dayalan Naidu S, Higgins M, Yamamoto M, Dinkova-Kostova AT, Kovac S, Abramov AY, Walker MC (2018) KEAP1 inhibition is neuroprotective and suppresses the development of epilepsy. Brain.141(5):1390-403.
61. Smith AM, Gibbons HM, Oldfield RL, Bergin PM, Mee EW, Faull RL, Dragunow M (2013) The transcription factor PU.1 is critical for viability and function of human brain microglia. Glia.61(6):929-42.
62. Spencer S, Huh L (2008) Outcomes of epilepsy surgery in adults and children. Lancet Neurol.7(6):525-37.
63. Staitieh BS, Fan X, Neveu W, Guidot DM (2015) Nrf2 regulates PU.1 expression and activity in the alveolar macrophage. Am J Physiol Lung Cell Mol Physiol.308(10):L1086-93.
64. Switon K, Kotulska K, Janusz-Kaminska A, Zmorzynska J, Jaworski J (2016) Tuberous sclerosis complex: From molecular biology to novel therapeutic approaches. Iubmb Life.68(12):955-62.
65. Terrone G, Balosso S, Pauletti A, Ravizza T, Vezzani A (2020) Inflammation and reactive oxygen species as disease modifiers in epilepsy. Neuropharmacology.167:107742.
66. Tucker ES, Segall S, Gopalakrishna D, Wu Y, Vernon M, Polleux F, Lamantia AS (2008) Molecular specification and patterning of progenitor cells in the lateral and medial ganglionic eminences. J Neurosci.28(38):9504-18.
67. Turkistany SA, DeKoter RP (2011) The transcription factor PU.1 is a critical regulator of cellular communication in the immune system. Arch Immunol Ther Exp (Warsz).59(6):431-40.
68. Uhlmann EJ, Wong M, Baldwin RL, Bajenaru ML, Onda H, Kwiatkowski DJ, Yamada K, Gutmann DH (2002) Astrocyte-specific TSC1 conditional knockout mice exhibit abnormal neuronal organization and seizures. Ann Neurol.52(3):285-96.
69. van Scheppingen J, Iyer AM, Prabowo AS, Muhlebner A, Anink JJ, Scholl T, Feucht M, Jansen FE, Spliet WG, Krsek P, Zamecnik J, Buccoliero AM, Giordano F, Genitori L, Kotulska K, Jozwiak S, Jaworski J, Liszewska E, van Vliet EA, Aronica E (2016) Expression of microRNAs miR21, miR146a, and miR155 in tuberous sclerosis complex cortical tubers and their regulation in human astrocytes and SEGA-derived cell cultures. Glia.64(6):1066-82.
70. van Scheppingen J, Mills JD, Zimmer TS, Broekaart DWM, Iori V, Bongaarts A, Anink JJ, Iyer AM, Korotkov A, Jansen FE, van Hecke W, Spliet WG, van Rijen PC, Baayen JC, Vezzani A, van Vliet EA, Aronica E (2018) miR147b: A novel key regulator of interleukin 1 beta-mediated inflammation in human astrocytes. Glia.66(5):1082-97.
71. van Vliet EA, Aronica E, Gorter JA (2015) Blood-brain barrier dysfunction, seizures and epilepsy. Semin Cell Dev Biol.38:26-34.
72. Verney C, Monier A, Fallet-Bianco C, Gressens P (2010) Early microglial colonization of the human forebrain and possible involvement in periventricular white-matter injury of preterm infants. J Anat.217(4):436-48.
73. Wang JH, Nichogiannopoulou A, Wu L, Sun L, Sharpe AH, Bigby M, Georgopoulos K (1996) Selective defects in the development of the fetal and adult lymphoid system in mice with an Ikaros null mutation. Immunity.5(6):537-49.
74. Wang Z, Nakayama Y, Tsuda S, Yamasu K (2018) The role of gastrulation brain homeobox 2 (gbx2) in the development of the ventral telencephalon in zebrafish embryos. Differentiation.99:28-40.
75. Yasin SA, Latak K, Becherini F, Ganapathi A, Miller K, Campos O, Picker SR, Bier N, Smith M, Thom M, Anderson G, Helen Cross J, Harkness W, Harding B, Jacques TS (2010) Balloon cells in human cortical dysplasia and tuberous sclerosis: isolation of a pathological progenitor-like cell. Acta Neuropathol.120(1):85-96.
76. Yu G, He QY (2016) ReactomePA: an R/Bioconductor package for reactome pathway analysis and visualization. Mol Biosyst.12(2):477-9.
77. Yu G, Wang LG, Han Y, He QY (2012) clusterProfiler: an R package for comparing biological themes among gene clusters. OMICS.16(5):284-7.
78. Zhang B, Zou J, Han L, Rensing N, Wong M (2016) Microglial activation during epileptogenesis in a mouse model of tuberous sclerosis complex. Epilepsia.57(8):1317-25.
79. Zhou N, Liu K, Sun Y, Cao Y, Yang J (2019) Transcriptional mechanism of IRF8 and PU.1 governs microglial

activation in neurodegenerative condition. Protein Cell.10(2):87-103.
80. Zimmer TS, Ciriminna G, Arena A, Anink JJ, Korotkov A, Jansen FE, van Hecke W, Spliet WG, van Rijen PC, Baayen JC, Idema S, Rensing NR, Wong M, Mills JD, van Vliet EA, Aronica E (2019) Chronic activation of anti-oxidant pathways and iron accumulation in epileptogenic malformations. Neuropathol Appl Neurobiol.
81. Zurolo E, Iyer A, Maroso M, Carbonell C, Anink JJ, Ravizza T, Fluiter K, Spliet WG, van Rijen PC, Vezzani A, Aronica E (2011) Activation of Toll-like receptor, RAGE and HMGB1 signalling in malformations of cortical development. Brain.134(Pt 4):1015-32.

Supplementary material

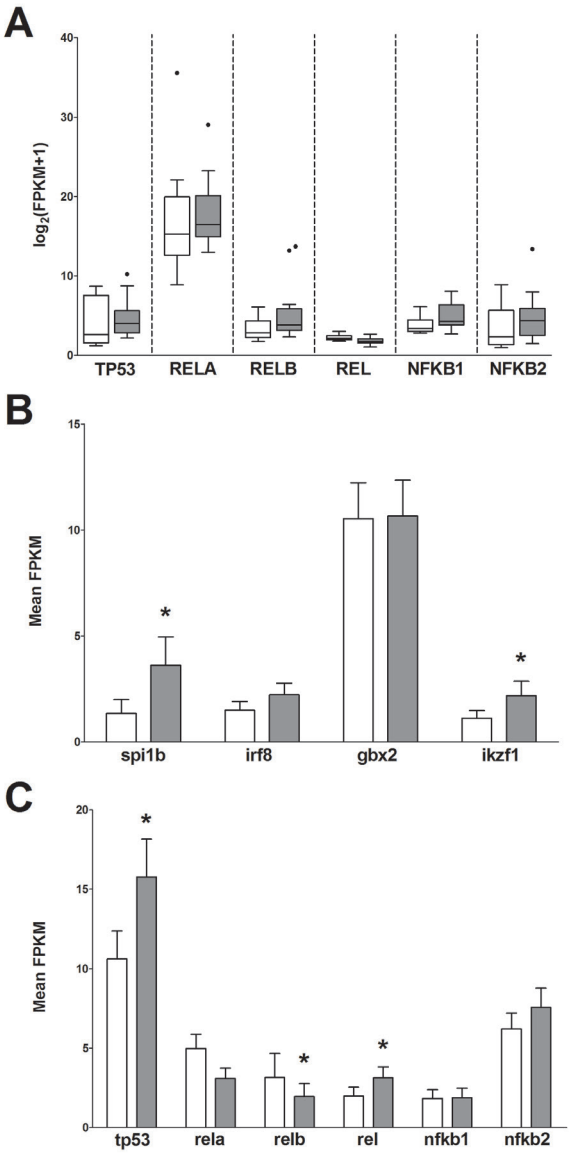

Supplementary Figure 1: Expression of transcriptional regulators in TSC cortical tubers and tsc2$^{-/-}$ zebrafish. Expression of TP53 and NF-κB subunits was not different between TSC tuber tissue compared to autopsy control (A). In zebrafish, the homologue spi1b and ikzf1 were higher compared to control fish, while irf8 and gbx2 were not different (B). Additionally, tp53 and rel expression were higher while relb expression was lower compared to control (C). A Data are expressed relative to expression in autopsy control and displayed as Tukey box plot. RNA-Seq n=10 autopsy control cortex samples (clear) vs. n=12 TSC cortical tubers (grey). B, C Data are expressed as bar graphs with SD. n=4 WT zebrafish (clear) versus n=3 *tsc2*$^{-/-}$ zebrafish (grey). * p<0.05, modified t-test.

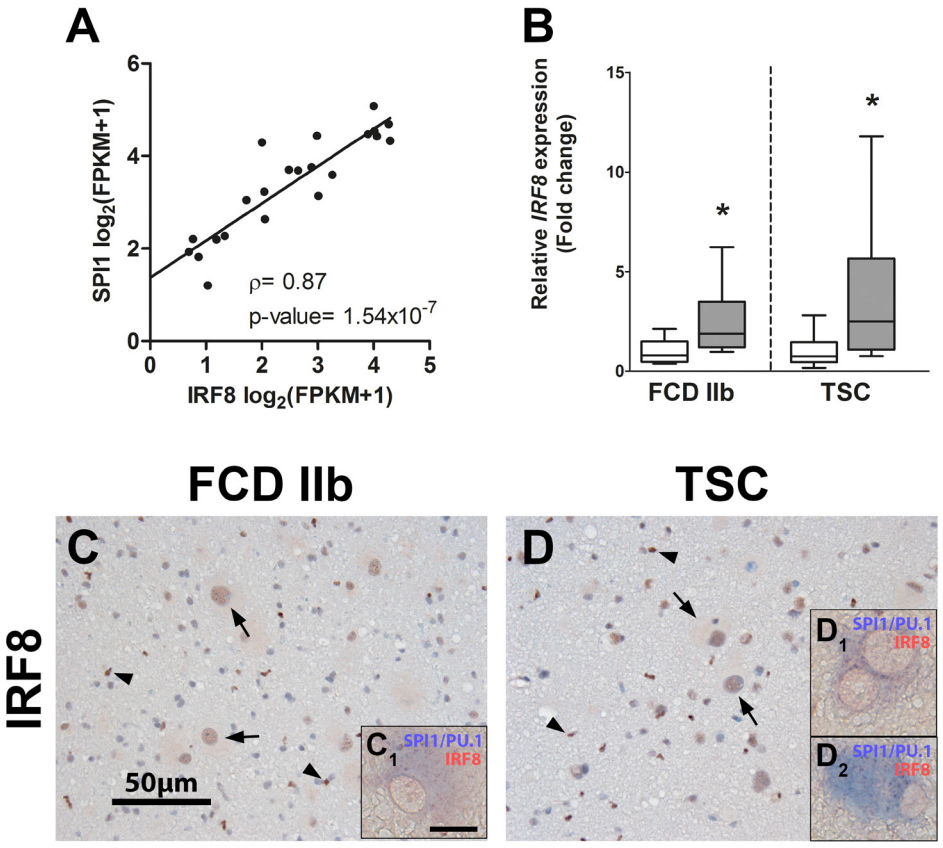

Supplementary Figure 2: IRF8 is increased in FCD IIb and TSC, and co-localizes with SPI1 in dysmorphic cells. SPI1 and IRF8 expression from RNA sequencing data display strong positive correlation (A). Total IRF8 expression was higher in FCD IIb tissue and a separate cohort of TSC (B). IRF8 expression was detected in the nucleus of microglia (arrowheads) and malformed cells (arrows) in FCD IIb and TSC tissue (C, D). IRF8 expression in giant and balloon cells was co-localized with cytoplasmic SPI/PU.1 expression (C_1, $D_{1,2}$). Sections C and D were counterstained with hematoxylin. Scale bars: 50 µm in C, 10 µm in C_1 (representative for inserts $B_{1,2}$), arrowheads = microglia, arrows = malformed cells. A Spearman's rank correlation test (displayed with Spearman correlation coefficient ρ and exact p-value). B Data are expressed relative to expression in autopsy control and displayed as Tukey box plot. Mann Whitney U-test. * $p<0.05$. A n=10 autopsy control cortex samples vs. n=12 TSC cortical tubers. B n = 8 autopsy control (for both FCD and TSC control groups) vs. n = 10 TSC and n=8 FCD IIb samples.

Suppl. Table 1: Clinical information of autopsy control tissue

Gender	Age (years)	Brain area
m	4	T
f	7 m	F
m	3	F
f	25	F
m	3.6 m	F
f	10	F
m	6 w	F
f	2	T, F
f	1	T
m	13	F
f	17	F
f	7 w	F
f	17	F
m	20	F
m	39	F
m	3 d	F
m	31	F
f	7	F
m	22 GW	F
f	21 GW	F
m	31 GW	F
f	0,9	T
f	2,5	F
m	15	F
f	1	T
m	10	F
f	39	F
f	44	F

Suppl. Table 2: Clinical information of FCD IIb and TSC tissue.

Pathology	Mutation	Gender	Age (years)	Duration epilepsy	Seizure types	Brain area	Seizures/ month	AEDs	Application
TSC	TSC1	m	8 m	5m	FS	F	>50	VGB	RNA
TSC	TSC2	m	2 y	1y	IS	F	-	VGB	RNA
TSC	TSC2	f	4 y	3y	FS, GS	F	>50	VGB	RNA
TSC	TSC2	m	2 y	2y	IS	F	-	VGB, CLB	RNA
TSC	TSC2	f	2 y	15m	GS	T	>50	VGB	RNA
TSC	TSC1	f	6 y	4y	FS	F	>50	VGB	RNA
TSC	TSC2	m	1 y	1y	IS	F	-	VGB, CLB	RNA
TSC	TSC2	f	3 y	2.5y	FS, GS	T	>50	VGB	RNA
TSC	TSC2	m	3 y	2.7y	FS	F	120	VGB	RNA
TSC	TSC2	m	8 m	8 m	FS	F	61	VGB, LEV, CLB	RNA
FCD IIb	-	m	41	40y	FA, FB/TC	F	122	CBZ, PGB, TPM, CLB	RNA
FCD IIb	MTOR	f	9	6 y	FIA, FB/TC	F	9	OXC	RNA/IHC
FCD IIb	MTOR	m	14	13y	FIA	F	457	VPA, PHT, LMT	RNA
FCD IIb	MTOR	m	5	2y	FIA, SE	F	152	VPA, VGB, PHT	RNA
FCD IIb	-	f	28	25y	FA, SE	F	304	PHT, CBZ, LMT	RNA
FCD IIb	-	m	14	10y	FA	F	213	LEV, LMT, CBZ	RNA
FCD IIb	-	m	21	14y	FIA, FB/TC	F	122	LEV, LCS, OXC, CNP	RNA
FCD IIb	MTOR	m	17	14y	FIA	F	122	LMT	RNA
FCD IIb	-	f	12	10y	FIA	F	356	VPA, CLB	IHC, ISH
FCD IIb	-	m	13	11.5	FIA, FB/TC	F	152	VPA, CBZ	IHC, ISH
TSC	TSC1	f	4 y	10m	FIA	F	600	PB, CLB, LEV, VGB, OXC, ZNS	IHC, ISH
TSC	-	m	13	13y	FIA, FB/TC	F	213	PHT, LEV	IHC, ISH
TSC	-	f	22	10y	FIA	F	609	CBZ, LEV, CLB, LMT	IHC, ISH
Fetal TSC	-	f	32 GW	-	-	F	-	-	IHC, ISH
Fetal TSC	-	m	23 GW	-	-	F	-	-	IHC, ISH
Fetal TSC	-	f	34 GW	-	-	F	-	-	IHC, ISH
TSC	TSC1	f	9	1y	FIA	F	122	OXC, CLB	Cell culture
TSC	TSC2	m	2	2y	FIA	F/P	304	LEV, VGB, PB, CLB	Cell culture
TSC	TSC2	m	2y	2y	FIA	F	152	ZNS	Cell culture
TSC	TSC2	f	13	13	FA	F	90	LTG, CBZ, CLB	RNA seq
TSC	TSC1	m	8	8	IS	F	90	LTG, CLB, TPM	RNA seq
TSC	TSC2	m	32	30	FA	T	>150	PHB, MDZ, LEV	RNA seq
TSC	TSC1	f	21	15	FB/TC	F	150-300	VPA	RNA seq
TSC	TSC1	m	0,9	0,8	FIA	T	150-300	CBZ, VPA, VGB	RNA seq
TSC	TSC2	f	10	10	FA	F	150-300	OXC, LTG	RNA seq
TSC	TSC2	m	47	35	FA,	T	>150	CBZ, CLB	RNA seq
TSC	TSC2	m	3	3	IS	F	120-300	VGB, LTG, CLB	RNA seq
TSC	TSC2	m	10	8	FIA	F	150-300	VPA, CLB	RNA seq
TSC	TSC2	f	1	0,83	FIA	F	240	VGB	RNA seq
TSC	TSC1	f	8	8	FIA	F	180	VGB, CBZ, VPA	RNA seq

TSC	TSC2	m	3	2	FA	T	180	VGB, LTG, CLB	RNA seq

m = male, f = female, FA = focal aware, FIA = focal impaired awareness, FB/TC = focal bilateral/tonic clonic, FS = focal seizure, GS = generalized seizure, IS = infantile spasms, F = frontal, T = temporal, P = parietal, CBZ = Carbamazepine, CLB = Clobazam, CNP = Clonazepam, LCS = Lacosamide, LEV = Levetiracetam, LMT = Lamotrigine, NP = Nitrazepam, PER = Perampanel, PGB = Pregabalin, PB = Phenobarbital, PHT = Phenytoin, OXC = Oxcarbazepine, TPM =Topiramate, VGB = Vigabatrin, VPA = Valproate

Suppl. Table 4: Primer sequences used for quantitative real-time PCR.

Species	Gene	Forward primer	Reverse primer
human	SPI1	CTCAGCAGTGATGGGGAGAG	CTGGAGCTCCGTGAAGTTGT
	IRF8	AGCATGTTCCGGATCCCTTG	CTGGTTCAGCTTTGTCCCCT
	GPx1	TTCCCGTGCAACCAGTTT	GGACGTACTTGAGGGAATTCTG
	SOD1	TCATCAATTTCGAGCAGAAGG	GCAGGCCTTCAGTCAGTCC
	TXNRD1	TTTCGACCCGGTCACACAAA	CAAACACAACGGGCAGATCG
	C1ORF43	GATTTCCCTGGGTTTCCAGT	ATTCGACTCTCCAGGGTTCA
	EF1α	ATCCACCTTTGGGTCGCTTT	CCGCAACTGTCTGTCTCATATCAC
mouse	Spi1	TCAGAGCTATACCAACGTCCAAT	GTGCGGAGAAATCCCAGTAGT
	Hprt-1	ATCACATTGTGGCCCTCTG	GTCATGGGAATGGATCTATCACT
	Tbp	GATGGGAATTCCAGGAGTCA	GAGAATCATGGACCAGAACA